Boiling and Evaporation in Small Diameter Channels

Arthur E. Bergles
abergles@aol.com

John H. Lienhard V
lienhard@mit.edu

Gail E. Kendall
gail@alum.mit.edu

Peter Griffith
pgrif@mit.edu

W.M. Rohsenow Heat and Mass Transfer Laboratory
Department of Mechanical Engineering
Massachusetts Institute of Technology
77 Massachusetts Avenue, Room 3-162
Cambridge MA 02139-4307

Abstract

Since the 1950's, the research and industrial communities have developed a body of experimental data and set of analytical tools and correlations for two-phase flow and heat transfer in passages having hydraulic diameter greater than about 6 mm. These tools include flow regime maps, pressure drop and heat transfer correlations, and critical heat flux limits, as well as strategies for robust thermal management of HVAC systems, electronics, and nuclear power plants. Designers of small systems with thermal management by phase change will need analogous tools to predict and optimize thermal behavior in the mesoscale and smaller sizes. Such systems include a wide range of devices for computation, measurement, and actuation in environments that range from office space to outer space as well as living systems. This paper examines important processes that must be considered when channel diameters decrease, including flow distribution issues in single, parallel, and split flows; flow instability in parallel passages; manufacturing tolerance effects; single-phase heat transfer; nucleation processes; boiling heat transfer and pressure drop; and wall conductance effects. The discussion focuses on engineering issues for the design of practical systems.

Introduction

Practical development of micro-devices is creating a need for better understanding of microscale transport phenomena. This is causing a worldwide redirection of transport research and development, from macroscale (conventional) to microscale situations. This transition has been going on for about 20 years. Significant differences in transport phenomena have been reported at the microscale as compared to the macroscale. Phase-change processes, particularly flow boiling, are important in the microscale, but relatively little work has been done in this area.

This brings up the question of a definition of size. Common language is not very helpful on this, as "micro" is not necessarily used to denote heat exchangers having feature sizes of 1 micrometer, but instead means "relatively small." For instance, "microturbines" have powers in the 50 kW – 75 kW range [1]. Many definitions of microscale hydraulic diameter are used in the literature. One of the most complete and consistent definitions is given in terms of hydraulic diameter D_h by Mehendale et al. [2]:

- micro heat exchangers: $D_h = 1 - 100 \, \mu$m
- meso heat exchangers: $D_h = 100 \, \mu$m – 1 mm,
- compact heat exchangers: $D_h = 1 - 6$ mm,
- conventional heat exchangers: $D_h > 6$ mm.

For purposes of the present review, considering the general lack of data on boiling in systems that are smaller than conventional, it is sufficient to simply designate the systems under consideration as "small."

Heat exchangers with small channels are generally subject to two problems that are encountered in conventional heat exchangers, but which are aggravated as channel size is reduced. The first of these is flow distribution among many parallel channels — a particularly serious concern with boiling flows. The second is conjugate effects, circumferential and axial heat conduction in the material forming the channel — so that the actual heat flux and temperature distributions at the channel wall are difficult to estimate.

Typical channels studied in the literature are rectangular, with one side unheated (usually a transparent cover plate in experimental apparatus) and heat is applied near the opposite wall, with the result that the heat flux and temperature are nonuniform circumferentially. Axial-conduction effects in the walls are also expected. Experimental channels are not normally instrumented to pick up these variations — if this is indeed possible.

The extent to which an incoming liquid will be vaporized is a design variable that depends upon the intended application. In microscale refrigeration systems, the change in vapor quality may be substantial, on the order of 0.8 for example. In electronics cooling applications, the equilibrium vapor quality may remain at 0, or be very small; in those designs, the aim is to capture the high heat transfer coefficients of subcooled flow boiling, without the added complexities of net vapor generation (e.g., the need to incorporate a condenser). The distinction between low and high quality outflow affects pressure drop, the potential for CHF, and the selection of the fluid inlet state.

The issue of nucleation is also crucial, if the favorable heat transfer characteristics of subcooled boiling are to be realized. In both of the above situations, there may be additional vapor generated (beyond that due to heat transfer at the wall) due to flashing that results from a severe pressure gradient.

Since work on this paper was initiated, several review papers have appeared that deal with microchannel heat transfer and pressure drop ([3, 4, 5, 6]). These papers confirm that this is indeed a "hot" topic. In order to avoid duplication, the present paper will focus primarily on issues not treated in the other review papers.

In this paper, we consider, in varying levels of detail, the general design trade-offs in small-diameter internal flow boiling, conjugate heat transfer, flow distribution, single-phase heat transfer, boiling inception, flow regimes, boiling heat transfer, enhancement, flow instabilities, and manufacturing issues.

Design Considerations

In some systems, small size alone may limit possibilities for thermal management systems based on phase change of a flowing fluid to very small channels. Moreover, available manufacturing methods may favor configurations that can be executed with relative simplicity in one dimension, confining complexities of flow configurations to the other two dimensions.

Here we ask the more general question of how to optimize thermal management when there is a range of possible flow configurations, including a range of possible flow channel diameters. We consider a general geometry that lends itself to relative simplicity in the vertical dimension in the sketch of Figure 1 below. The sketch shows a rectangular solid, heated (uniformly) on one side, and perforated by one or more rows of identical channels parallel to the heated surface. The solid in Figure 1 can be thought of as a stack of plates, some with slots for the channels, and some solid. Several possible patterns and channel sizes (D_1, D_2,...) are shown for illustration, although in the following we shall assume that only one channel pattern is used in any particular case. The channels may be connected at the ends to form lengths of $L = 2H$, $3H$ or more; or the channels may be divided in mid-block, to form flow lengths of $L = H/2$, $H/3$ or less. Let the ratio of channel length to block length be $r = L/H$.

A General Design Problem

The design question we pose is: *given* the heat rate Q (W), the length (and width) H, *select* a working fluid, its mass flow rate M (kg/s), the channel dimension D, the channel length L, the channel spacing $S \cdot D$ (for S a number > 1), the number of channels n, and the material and thickness of the block, W. We will be particularly interested in the pumping power P (W) and material thickness W.

We first observe that the width and thickness of the block, and the number, length, diameter, and spacing of the channels are not independent. Our geometric configuration requires that the number of channels in a row, n_c, be

$$n_c = \frac{H}{SD} \tag{1}$$

and that the number of rows of channels is

$$n_r = \frac{W}{SD} \tag{2}$$

The total number of holes in a cross section, which is the number of channels, is

$$n = n_c n_r = \frac{WH}{(SD)^2} \tag{3}$$

And the summed length of all channels is given by

$$nL = n\, rH = r\, \frac{WH^2}{(SD)^2} \tag{4}$$

We also observe that n must be an integer (i.e., $n = 1, 2, 3 \ldots$) and that channel flow is characterized by lengths that are at least several diameters in magnitude. The latter constraint does not prelude operation in the "entry length" mode.

General Design Guidelines

There are several other constraints due to transport processes for energy, heat, and momentum. Below we will consider the steady-state operating conditions, but not start-up or shutdown conditions. First, we note that in a phase-change-controlled thermal management system, the energy associated with phase change will account for the majority of the heat removal

$$Q = M \Delta x\, h_{lg} \tag{5}$$

where Δx is the change in quality over the length of the channel and h_{lg} is the latent heat of vaporization for the coolant. For applications where the entire channel is in the subcooled boiling mode there would be no change in equilibrium quality. In this case, the total heat removal might be on the order of that needed to bring the coolant to saturation temperature:

$$Q \approx M c_{p_l}(T_{\text{sat}} - T_{\text{sub}}) \tag{6}$$

where c_{p_l} is the specific heat of the liquid coolant, T_{sat} is the saturation temperature, and T_{sub} is the inlet temperature of the subcooled coolant. Given a desired value of Δx (whether low or high) or of $(T_{\text{sat}} - T_{\text{sub}})$, Eq. 5 or 6 can be used to get a first estimate for the mass flow rate of coolant at the system pressure.

  Employing an overall energy balance for the square channels with sides of length $D_1 \equiv D$, we obtain

$$Q = 4D\, nL\, q = \frac{4rWH^2}{S^2 D}\, q \tag{7}$$

where q is the average heat flux at the channel wall. In the case of circular channels of the same diameter D, π would replace the number 4 in this equation.

  Next, we require that the average heat flux be bounded by the critical heat flux (CHF) for the flow, in order to avoid excessive temperatures in the solid, or

$$q < q_{\text{CHF}} \tag{8}$$

where q_{CHF} is the CHF. It is important to note here that the CHF depends on the flow conditions, including the mass flux and the vapor quality. Using Eq. (7) to eliminate q, we find

$$q_{\text{CHF}} > \frac{QS^2D}{4rWH^2} \tag{9}$$

In order that the lower heat transfer surfaces in Figure 1 will contribute to energy transport, the solid should be an effective conductor of heat through its thickness. In other words, conjugate heat transfer effects (discussed in greater detail in the next section of this paper) should not offer a significant resistance to heat flow in comparison with that of the fluid in the channel. Since the heat transfer coefficient is generally a maximum at CHF, this leads to

$$\frac{k_{\text{solid}}(S-1)}{4W} \gg \frac{q_{\text{CHF}}}{(T_{\text{CHF}} - T_{\text{sat}})} > \frac{q}{(T_{\text{CHF}} - T_{\text{sat}})} \tag{10}$$

where k_{solid} is the thermal conductivity of the solid, and T_{CHF} and T_{sat} are the wall temperature at critical heat flux and the saturation temperature of the fluid, respectively. Substituting Eq. (7) into Eq. (10), we obtain

$$\frac{k_{\text{solid}}(S-1)}{W} \gg \frac{Q}{rnLD(T_{\text{CHF}} - T_{\text{sat}})} \tag{11}$$

Next we observe that a good design will be one in which the pumping power P is small compared to the heat removal rate Q:

$$P \ll Q \tag{12}$$

Pumping power, in turn, depends on the pressure drop through the channel, Δp.

The issue of pressure drop in small channels is a subject of research for both single- and two-phase flows. Here we will refer to conventional analysis of pressure drop in two-phase flow to see what insight we might gain. In a flow boiling situation, the pressure gradient is typically expressed in relation to the single-phase liquid pressure gradient at the same mass flux. Here we consider the case of no change in channel elevation over its length, and negligible pressure drop due to the acceleration of the vapor phase. The pressure drop along the channel is then the sum of the pressure drop at the entrance and the frictional pressure drop along the channel:

$$\Delta p = \Delta p_{\text{ent}} + \Delta p_{\text{fr}} \tag{13}$$

The pressure drop for the entrance is generally given in terms of a dimensionless entrance loss coefficient. However, orifices are often used at the entrances of parallel two-phase channels in order to maintain flow stability. In this case, the orifices are sized such that the pressure drop at the entrance is proportional to the pressure drop in the rest of the channel.

$$\Delta p = (1 + C)\Delta p_{\text{fr}} \tag{14}$$

The proportionality constant C is typically in the range of 1/3 to 2/3. The two-phase pressure gradient along the length of the channel is typically expressed in terms of the pressure gradient expected for the same flow rate of single-phase liquid through the same channel

$$\frac{dp_{\text{fr}}}{dz} = \Phi_l \frac{dp_{\text{lo}}}{dz} \tag{15}$$

5

where dp_{fr}/dz is the frictional two-phase pressure gradient in the axial direction z, dp_{lo}/dz is the pressure gradient in a single-phase liquid flowing through the same size channel at the same mass flow rate, and Φ_l is the ratio of two-phase frictional pressure gradient to single-phase liquid frictional pressure gradient [7]. The correction factor Φ_l depends very much on the vapor quality of the flow, and, therefore, in a flow boiling channel it varies considerably along the length. Here we use a channel average, $\overline{\Phi}_l$, to express the overall pressure drop in the channel:

$$\Delta p = (1 + C)\overline{\Phi}_l \Delta p_{\text{lo}} \tag{16}$$

The single-phase pressure drop over the length of the channel is given by

$$\Delta p_{\text{lo}} = \frac{M^2}{2\rho_l n^2 D^4} \left(\frac{fL}{D}\right) \tag{17}$$

where f is the Darcy friction factor, which depends on the Reynolds number.

Pressure drop can be estimated as the product of the volumetric flow rate (M/ρ) (m^3/s) and the pressure drop through the channel, Δp, when the flow quality remains low:

$$P = \frac{M\Delta p}{\rho_l} \tag{18}$$

Thus the required pumping power can be expressed in terms of the mass flow rate and other variables as follows:

$$P = \frac{M^3(1 + C)fL\overline{\Phi}_l}{2\rho_l^2 n^2 D^5} \tag{19}$$

We can substitute Eqs. (19) and (3) into Eq. (12) and rearrange to find a requirement on the channel size D:

$$D \gg \frac{M^3(1 + C)f\overline{\Phi}_l}{2\rho_l^2 Q} \frac{S^4 L}{H^2 W^2} \tag{20}$$

The variation of the two-phase friction factors, for the case of large quality change, is discussed by Kandlikar [3]. Various measurements of two-phase flow pressure loss in microchannels are summarized in [4]. As one specific example, Bowers and Mudawar [8] were able to predict their microchannel pressure-drop measurements to within $\pm 30\%$ using the homogeneous flow model.

We now have 5 design constraints, but 6 unknowns plus two materials (one fluid, one solid) to select. We examine what they suggest so far. The first constraint, Eq. (4), is purely geometric. The second constraint, Eq. (5) or (6), suggests a high value for latent heat of evaporation of the coolant or adequate subcooling. The third, Eq. (8) or (9), suggests a high value for the critical heat flux, and a high surface area for heat transfer. The fourth, Eq. (10) or (11), suggests a high value for the solid thermal conductivity. These four are all compatible and consistent with heat exchanger design in general. We also bear in mind that, for a given mass flux (mass flow rate per unit flow area), the critical heat flux rises significantly with decreasing channel diameter, as discussed in more detail in another section of this paper. This trend is further enhanced by the higher surface area per unit flow area with smaller diameters. Therefore, the total heat transfer area needed decreases with channel diameter. The final constraint, Eq. (12), presents a more serious limitation as diameter decreases: the larger surface area per unit flow area with smaller diameters can also mean more surface drag and a higher pumping power. The various trade-offs are explored further in the following example.

Example of Channel Size Reduction

Suppose that an acceptable design has been made using square channels of size D_1 in a single row, i.e., $n_r = W/(D_1 S) = 1$. Let us examine the consequences of trying to manage the same heat flow, Q, with a much smaller diameter channel D_2 (e.g., $D_1 = 10 D_2$) while keeping the same fluid, solid, and heat load area (HL). We are particularly interested in the trade-off between thickness W of the solid, and the pumping power P required for the coolant. This exercise is similar in nature to the analysis presented by Palm [9] for heat exchangers. Owing to the different constraints imposed here, however, the results are different.

If both cases are designed to the same ratio of average heat flux to critical heat flux, the CHF constraint of Eq. (9) suggests that

$$q_{\text{CHF},2} \frac{4 W_2 H_2^2 r_2}{S_2^2 D_2} \approx q_{\text{CHF},1} \frac{4 W_1 H_1^2 r_1}{S_2^2 D_1} \tag{21}$$

or, since $H^2 r = HL$ is held constant,

$$\frac{W_2}{W_1} \approx \frac{q_{\text{CHF},1}}{q_{\text{CHF},2}} \frac{S_2^2 D_2}{S_1^2 D_1} \tag{22}$$

That is, we may expect some savings in material thickness by going to a smaller diameter. The savings will be more extreme than the diameter ratio alone because of the dependence of q_{CHF} on channel diameter. A reduction of diameter by a factor of 10, for example, might result in a reduction of thickness of up to 100, if the mass fluxes are the same in both cases. We note from Eq. (10) that if the solid was an adequate conductor for case 1, it is likely to be adequate in case 2 as well.

Now we can estimate ratio of total channel length in the two cases using Eq. (4).

$$\frac{n_2 L_2}{n_1 L_1} = \frac{W_2 H_2^2 r_2}{W_1 H_1^2 r_1} \frac{(S_1 D_1)^2}{(S_2 D_2)^2} \approx \frac{q_{\text{CHF},1}}{q_{\text{CHF},2}} \frac{D_1}{D_2} \tag{23}$$

So, if the critical heat flux varies as the inverse of channel diameter, our result matches that of Palm [9], i.e., the products of number and length of channels in the two cases are equal.

We seem to have some flexibility to choose many short channels, or fewer long channels, as long as we get the total heat transfer area required. Let us now consider variation of the channel length, assuming that both the total mass flow rate and the mass flux are held constant. In particular, we hold mass flux constant because critical heat flux depends on mass flux. If both the mass flux and the mass flow rate are the same in both cases, then the flow areas must be the same:

$$n_1 D_1^2 = n_2 D_2^2 \tag{24}$$

or

$$\frac{n_2}{n_1} = \frac{D_1^2}{D_2^2} \tag{25}$$

If $D_1 = 10D_2$ as above, the number of channels will increase by a factor of 100. Substituting Eq. (25) into Eq. (23) gives the ratio of the channel lengths for a constant mass flux:

$$\frac{L_2}{L_1} \approx \frac{q_{\text{CHF},1}}{q_{\text{CHF},2}} \frac{D_2}{D_1} \tag{26}$$

For the constant mass flux case, then, if the critical heat flux varies as the inverse of diameter, the channel lengths for the smaller channels of case 2 will be shorter than the channel lengths of case 1 by a factor of 100.

Finally, we can consider how the change in channel size affects the pumping power for low quality flows. The ratio of the pumping power requirements, from Eq. (19), is:

$$\frac{P_2}{P_1} \approx \frac{(1 + C_2)f_2\overline{\Phi}_{l2}}{(1 + C_1)f_1\overline{\Phi}_{l1}} \frac{n_1^2 D_1^5}{n_2^2 D_2^5} \frac{L_1}{L_2} \tag{27}$$

If we then substitute Eqs. (25) and (26), we find

$$\frac{P_2}{P_1} \approx \frac{(1 + C_2)\overline{\Phi}_{l2}}{(1 + C_1)\overline{\Phi}_{l1}} \frac{f_2}{f_1} \frac{q_{\text{CHF},1}}{q_{\text{CHF},2}} \tag{28}$$

The orifice coefficients, C_1 and C_2, will have similar design values in both cases, and for low quality flow, $\overline{\Phi}_l$ will be of order one. With the same mass fluxes, we get comparable velocities, and the Reynolds numbers will depend only on diameters. The friction factor varies roughly as the $-1/4$ power of Reynolds number, from the Blasius friction formula. If the critical heat flux varies as the inverse of channel size, then the pumping power ratio is proportional to $(D_2/D_1)^{3/4}$. For the ten-to-one size ratio considered here, this means the pumping power will be 5.6 times *lower*, owing mainly to the much higher CHF in the smaller diameter channel. A pumping power ratio of 1 was imposed by Palm [9] in his analysis, which yielded a constant mass flux in the case of laminar flow, in which the heat transfer coefficient varies inversely with diameter.

Therefore, if we have found a good solution at D_1, there exists a similar solution with the same mass flux at a smaller diameter D_2, with savings in material thickness W with a substantial reduction in pumping power P. By raising the mass flux for the smaller diameter case, we might achieve further reductions in W (down towards its lower limit of approximately $D_2 \times S$), with less reduction of P. The smaller system will have a very large number of parallel channels of relatively short length, as compared with the larger system.

Implications of Design Constraints

The simplified relations developed above give some small indication of: (i) the role of the conjugate heat transfer effects (particularly considering the non-uniformity of heat flow around the perimeter of the channels in the examples used); (ii) the significance of the dependence of CHF on flow rate; and (iii) the critical necessity of achieving uniform division of flow in what may turn out to be a large number of parallel channels. These issues will be discussed in the following sections.

Conjugate Heat Transfer Effects

Decreases in the size of the system may alter the relative importance of conduction resistance in the heat transfer surface. This is of concern both for critical heat flux (CHF) processes and for calculation of the heat transfer rate into the liquid in the single-phase and flow boiling regimes of the passage.

With sufficient heat addition, critical heat flux conditions may be reached at some point in the duct. If the corresponding heat flux is sufficiently high, melting of the wall (i.e., burnout) may occur in locations that become dry. These fluxes are more likely to be reached in electronics cooling applications than in HVAC equipment. Owing to the small size of the channels, however, it is possible that azimuthal conduction may limit the temperature rise possible in any locally dry parts of the perimeter. Axial conduction will do the same for full dry regions of the tube.

For single-phase flow or subcooled boiling, conjugate effects will be related to both entry region effects, where locally high h may lead to heat conduction away from low h regions, and also geometrical effects by which conduction resistance will reduce heat flow to parts of the channel perimeter that are more distant from the heat source.

To assess these conjugate effects, we shall consider first a two-dimensional situation in which the flow has stratified, as a model for conjugate effects preceding burnout. We next consider two-dimensional situations appropriate to single-phase convection or subcooled boiling, with the objective of seeing whether conjugate effects should be expected on a local basis. Finally, we discuss the role of axial variations in h and T, the three-dimensional problem.

We note that, for tubes whose dimensions approach the mean-free-path of the energy carriers in the solid (typically well below one micrometer), microscale heat conduction effects may raise the thermal resistance further [10]. These true microscale effects are not considered here.

Conduction Resistance in 2D Stratified Flow

Let us consider a representative geometry with a row of parallel tubes embedded in a solid surface that is heated on its upper face and adiabatic below (Figure 2). To estimate the potential for conjugate effects to limit CHF phenomena, we examine a hypothetical situation of stratified flow in which the lower half of the tube is filled with liquid and the upper half with vapor.* Both liquid and vapor have the local bulk temperature T_b. The liquid and vapor phases have heat transfer coefficients h_{liq} and h_{vap}, respectively. Circular tubes are considered for convenience, although it is recognized that they will be difficult to manufacture in very small diameters. Three aspect ratios characterize this arrangement:, W/D, W_b/D, S. From symmetry, it is adequate to consider just one cell of width $S \cdot D$ having adiabatic vertical sides (Figure 2). The upper surface may be modeled as having a specified heat flux, q_0, or a specified temperature, T_0.

Under both top surface boundary conditions, the highest temperature on the interior of the tube, T_{max}, will normally occur at the top center. Under the fixed flux condition, the upper surface of the solid will have a nonuniform temperature. If the tubes are not

---

*We say hypothetical because some evidence suggests that the stratified regime becomes less important as diameter decreases.

too far apart, the maximum surface temperature, T_{sx}, will lie directly above the center of the tube; but, for large tube spacings, it may lie between the tubes at the edge of the cell. For burnout considerations, $(T_{max} - T_b)$ is the temperature difference of interest. From examination of the steady heat conduction equation in the solid, it follows that

$$\left(\frac{T_{max} - T_b}{T_0 - T_b} \right) = f \left(\text{Bi}_{vap} = \frac{h_{vap}D}{k_{solid}}, \text{Bi}_{liq} = \frac{h_{liq}D}{k_{solid}}, \frac{W}{D}, \frac{W_b}{D}, S \right) \tag{29}$$

in the fixed T_0 case, and

$$\frac{T_{max} - T_b}{(q_0 W/k_{solid})} = f \left(\text{Bi}_{vap}, \text{Bi}_{liq}, \frac{W}{D}, \frac{W_b}{D}, S \right) \tag{30}$$

in the fixed q_0 case, where $(T_{max} - T_b)$, is clearly on the order of $q_0 W/k_{solid}$, if the other parameters are fixed. The highest values of T_{max} correspond to $h_{vap} \to 0$; the largest azimuthal differences in temperature correspond to $h_{vap} \to 0$ with $h_{liq} \to \infty$. In this limit, the upper surface of the tube is adiabatic and the lower surface is isothermal at T_b. Moreover, in this limit, all thermal resistance is conductive and the size of the resulting azimuthal temperature difference, $(T_{max} - T_b)$, is controlled by the aspect ratios. For example, the fixed flux case becomes

$$\frac{T_{max} - T_b}{(q_0 W/k_{solid})} = f \left(\frac{W}{D}, \frac{W_b}{D}, S \right) \tag{31}$$

The evaluation of these geometrical, heat conduction effects pose no particular technical difficulties and are not a small channel issue *per se.*

It is obvious that the largest differences occur as $S \to 1$, since the conduction resistance between the adiabatic tube top and the cooled tube bottom becomes very large when the tubes are tightly spaced. The limits $W \to D$ and $W_b \to D/2$ are also unfavorable in that they increase the conduction resistance in the vicinity of the top and/or bottom center of the tube's interior surface.

Finite-element simulations of the heat conduction were run for $W = S \times D$, $W_b = W/2$, and several values of D/W. Dimensionless azimuthal temperature differences are given in Table 1 using the nondimensionalizations indicated in Eqs. (29) and (30). The computations are based on steady two-dimensional conduction using a linear triangular element and are intended to represent trends; they are accurate to approximately the number of digits given.

Similar results have been published by Bowers and Mudawar [11] for circular tubes having an entirely isothermal tube surface. They report that the tube pitch S should be less than 2, while the ratio W/D should be no less than 1.2 for structural reasons.

Two-Dimensional Conduction Effects for Homogeneous Flow

The preceding discussion concerned the conductive limit of the two-phase problem, but the true conjugate problem will arise when $\text{Bi}_{vap} > 0$ and $\text{Bi}_{liq} < \infty$. We now consider two-dimensional cases in which flow field is homogeneous. This situation is representative of single-phase flow and subcooled flow boiling. With the proper choice of h, it might also describe intermittent flow or misty flow.

An initial concern is the size of the Biot number, $\text{Bi} = hD/k_{\text{solid}}$. The use of this Biot number presumes that conduction resistance is adequately characterized by D/k_{solid}, a presumption we revisit momentarily. For an initially single-phase state, either a laminar or a turbulent flow may prevail.

For fully developed laminar flow, $h_{\text{lam}} = \beta k_{\text{fluid}}/D$, where β is a constant that depends on channel shape and thermal boundary condition, typically between 3 and 8. The Biot number is then equal to $\beta(k_{\text{fluid}}/k_{\text{solid}})$. For typical solid-fluid combinations (water/silicon, for example), this leads to a Biot number much less than unity and negligible conduction resistance and wall temperature variation. (If a liquid metal coolant is being used, of course, this conclusion must be revisited.)

Turbulent flow becomes less likely with the decreasing channel size owing to the very high-pressure drop required to generate high Reynolds number. Nevertheless, turbulent Nusselt numbers may be accurately calculated from the Gnielinski equation for small diameter fully developed tube flows having Reynolds numbers above transition. The Biot number is again $\text{Bi} = \text{Nu}_D(k_{\text{fluid}}/k_{\text{solid}})$. If we consider room temperature water flowing at a Reynolds number of 6000, we would find Nu_D of about 50, corresponding to Bi of about 0.2 for a silicon substrate. At this Bi, conduction effects are no longer entirely negligible. This condition corresponds to a 1 mm tube carrying water at 6 m/s with 6.5 kPa/cm pressure gradient. To the extent that turbulent convection Nusselt numbers are representative of subcooled flow boiling Nusselt numbers, an identical conclusion applies to the latter case.

The premise that D/k_{solid} describes the conduction resistance may fail in other geometries. For example, for channels separated by thin vertical sections (see Figure 3), the primary conduction length scale is the channel height, W_c, rather than the channel hydraulic diameter, D_h. The conduction resistance will be higher than D_h/k_{solid} indicates.

A number of studies have assessed the role of conduction in the walls of deep rectangular channels. The simplest approximation is to model the vertical wall between the channels using a one-dimensional fin approximation and to treat h as if uniform around the channel perimeter at each axial location. As noted by Phillips [12], these approximations have been found by many investigators to work well in predicting measured performance, provided that the fin efficiency is above about 80%; Kadle and Sparrow [13] drew similar conclusions in a comparison of full-numerical, experimental, and one-dimensional results.

One-dimensional fin models are discussed in any undergraduate textbook [14]. The appropriate parameter to characterize the conductive resistance in the vertical walls is then the fin parameter, m:

$$mW_c = \left(\frac{h \cdot 2H}{k_{\text{solid}} \cdot Ht_s} \right)^{1/2} W_c \tag{32}$$

where t_s is the thickness of the fin. When mW_c is less than about 0.4, the fin efficiency will exceed 95% and fin effects can be neglected to a first approximation. In our particular case, if we suppose that we have fully developed laminar flow, then $h = \beta k_{\text{fluid}}/D_h$, for an appropriate β and hydraulic diameter. The fin parameter becomes

$$mW_c = \left(\frac{2\beta k_{\text{fluid}}}{k_{\text{solid}} t_s D_h} \right)^{1/2} W_c = \left(\frac{k_{\text{fluid}}}{k_{\text{solid}}} \right)^{1/2} \left(\frac{2\beta W_c^2}{t_s D_h} \right)^{1/2} \tag{33}$$

11

A calculation shows that, with typical conductivity ratios of 0.01, β near 8, t_s approximately equal to t_c (thickness of the channel), and hydraulic diameters on the order of $2t_c$, fin effects cannot be neglected unless W_c/t_s is less than about 1.4. We can see that fin effects will matter in most cases of thin rectangular channels. If one-dimensional models of this type are applied, however, other thermal resistances must also be carefully accounted for, as described in some detail by Phillips et al. [15].

Optimization of the thickness, t_s, height, W_c, and channel width, t_c, will depend upon the application of additional constraints. Phillips [12], for example, discusses optimization in the case of a fixed base area of the fin, $t_s W_c$. Phillips et al. [15] describe a numerical optimization on many variables. One significant finding was that it is advantageous to use relatively large channel widths (perhaps 200 to 300 μm) for water-cooled semiconductors, rather than the smaller dimensions that had been suggested in the earlier work of Tuckerman and Pease [16]. The principal reason for this was that turbulent flow could be achieved in those passages with modest pressure drop; this raises h significantly, thus cutting the dominant thermal resistance in the heat sink. It should also shorten the region of developing flow.

Conjugate Effects Associated with Axial Variations

For many microchannel arrangements, the flow field will be laminar and will, therefore, have a long entry length. Consequently, a substantial part of the passage may be in the developing flow regime. The low convection resistance near the inlet to the channel may then promote heat conduction through the solid surfaces toward the inlet.

Study of these problems in connection with microchannels began in the 1980's. Several authors have recently examined such effects using 3D numerical simulations of the coupled laminar flow and conduction problems for water-cooled silicon heat sinks [17, 18]. These authors considered relatively small rectangular passage sizes (in the range of $50 - 100\,\mu$m), for which the flow is laminar and in which fin effects in the channel walls are significant. Fedorov and Viskanta [18] report a substantial developing flow effect in the channels, so that simple Poiseuille flow cannot be used to model the pressure drop and heat transport. Their results further indicate that heat may actually flow out of the liquid in the corners of the channel back into the solid. The latter effect is a direct result of the low Biot number: the walls may provide a lower thermal-resistance path to the interior of a rectangular channel than does convection from a remote corner of the liquid toward the channel core.

In general, a small system with the same geometric proportions and materials as a larger one will experience similar conjugate heat transfer effects, due to the combined effects of the shorter heat transfer path in the solid, and the larger heat transfer coefficients in the fluid phase.

Summary of Conjugate Effects

As the passage size is reduced, heat transfer coefficients rise, but conjugate effects are a stronger function of the design geometry. Conjugate heat transfer effects will occur when too little material separates adjacent passages, if the flow is stratified or if the passages have fin-like separators. Under these conditions, heating will increasingly

show a one-sided character, and both heat transfer coefficients and pressure drop will be affected considerably. These geometric effects can be designed out, if desired, and are not intrinsic to the use of small-diameter passages.

Flow Distribution

For a single-phase flow or a subcooled boiling flow, the established methods described in [19], for instance, are applicable as long as the pressure drop can be predicted. In-so-far as using a two-phase flow at the inlet of an array of small diameter cooling channels, the development of microchannel evaporators will require an enabling technology: a small-scale refrigerant distributor that will ensure uniform flow/quality to each channel. These methods can also be used for a cooling system that incorporates subcooled boiling.

For a system that uses a saturated, two-phase mixture as a coolant, special care must be taken to ensure that the two phases, particularly the liquid, are properly distributed. There are two established ways of doing this [20, 21, 22, 23]. The simplest is a cascade of "tee's" into which the two-phase flow is admitted and emerges as two streams with the same quality (see Fig. 4a). This is repeated for each of the emerging streams until the requisite number of streams is obtained. The inconvenient aspect of this is that the number of emerging streams has to be a power of 2. Such an array of flow splitting "tee's" can easily be fabricated using the procedures used to fabricate the rest of the cooling systems. This is an attractive feature.

The second possibility uses an array of throttles and capillary tubes, which are rotationally symmetrical (see Fig. 4b). The flow passes through a throttle and emerges as a two-phase flow in a tube. That tube terminates at a second throttle formed by the gap between a flat surface and the end of the first throttle exit tube. Arranged around a second throttle is a circular array of capillary tubes, which conveys the two-phase mixture through a plenum to the cooling passages. Any number of tubes can be accommodated.

For these distributors, manufacturing tolerances dominate the performance uncertainties. For sufficiently small Weber number, surface tension may also affect performance. For sufficiently large Froude number, the orientation relative to gravity is unimportant. In most cases, flow distributors are relatively large components. Tests are now underway to assess two-phase distributors for evaporator tubes [24, 25].

Single-phase Heat Transfer Coefficients

Although some concerns have been raised in the literature about the viability of standard, continuum internal flow results in small channels, physical considerations strongly suggest that the usual conservation equations will apply for liquids in any tube whose diameter is large compared to molecular scales. Entry effects must be accounted for and manufacturing tolerances must be taken into account. In a post-dryout region, continuum theory can be expected to apply in the vapor phase for channel sizes greater than 10 or so mean free paths, typically implying micrometer diameters [26]. In the absence of such effects, however, a recent survey by Obot [27] concluded that conventional relationships are applicable to microchannels. Obot's comparison of a number

of microchannel heat transfer measurements to conventional scalings, shown in Fig. 5, indicate significant differences from conventional correlations. The turbulent data are generally higher than the conventional correlation, and an unexpected Reynolds number dependence appears in the *laminar* range. Sobhan and Garimella [28] found existing "microchannel" friction and heat transfer predictions to produce mutually contradictory results in both regimes, which, in effect, confirms Obot's conclusion about conventional correlations being acceptable on the average.

Several recent studies have compared careful measurements of pressure loss or velocity profiles for liquids flowing in microchannels to standard results [29, 30, 31]; agreement is excellent down to hydraulic diameters of 75 μm or so. While some deviations have been reported in smaller channels, no new physical phenomena have been identified. It must be emphasized that accurate experimentation on such small channels is very difficult — particularly measurements of fluid or wall temperatures and fluid enthalpy changes.

A few conventional issues gain much greater importance to heat transfer heat transfer coefficients for small diameter passages. First, since many of the configurations of interest will involve some variation of temperature and heat flux around the channel perimeter, wall boundary conditions may be non-uniform.

Second, as was noted previously, Fedorov and Viskanta [18] showed that small channels, which are often characterized by laminar flow, may have significant portions in the developing flow regime. Entry-length effects must therefore be considered in evaluating both heat transfer coefficients and pressure drop. Kandlikar et al. [32] have recently shown the standard entry length correlations for the thermally-developing region of a hydrodynamically fully-developed flow to be within experimental error in tubes of 0.6 and 1 mm diameter.

A third issue is wall roughness. Kandlikar et al. [32] have shown that wall roughness can significantly affect heat transfer, pressure drop, and transition Reynolds number in small tubes. Study in this area is continuing, but it is to be noted that a level of roughness that is negligible in a large tube may be significant in a tiny tube. This matter is related to the overall issue of manufacturing tolerances, which may potentially alter hydraulic diameters or produce local orificing; such effects will obviously compromise the accuracy of any effort to predict single-phase flow characteristics in small diameter channels.

A fourth issue, which applies to only gas flows, is compressibility [33]. These effects can be treated using the techniques of compressible flow theory [34], particularly those for low Mach number channel flows.

A final issue is viscous dissipation. A number of authors have suggested that dissipation may be responsible for some reported anomolies in small channel heat transfer coefficients (e.g., [35]), so a more extended discussion is in order. At the outset, it should be noted that dissipative heat generation has approximately the same variation with diameter as the heat transfer coefficient: it therefore does not take on special significance in small diameter tubes. Nevertheless, if large pressure gradients are imposed on a small diameter tube, significant viscous heating can occur, altering the temperature profiles in the channel. It is instructive to start by thinking of an adiabatic tube.

For adiabatic channel flow with viscous heating, the bulk enthalpy, h_b, remains constant along the length of the tube while pressure drops and entropy rises. For an ideal

gas, this means that the bulk temperature also remains constant ($dh_b = c_p dT_b = 0$), whereas for an incompressible liquid, the bulk temperature rises ($dh_b = c_{p_l} dT_b + dp/\rho_l = 0$). In both cases, the major effect of dissipation is to raise the fluid temperature near the wall, resulting in an adiabatic wall temperature greater than the bulk temperature, $T_{\text{aw}} > T_b$. In general, the difference between these two temperatures varies as $\Pr(u_b^2/2c_p)$.[†]

When significant dissipation is present in a non-adiabatic tube, the heat flux should be calculated in terms of the difference between the wall temperature and the adiabatic wall temperature: $q = h(T_w - T_{\text{aw}})$. When this is done, h itself may be calculated using standard results for non-dissipative flow, as follows from superposition and as was verified experimentally before 1950 [36, 34]. Unfortunately, a substantial number of papers published after 1960 have based h for dissipative flow on $(T_w - T_b)$, creating strangely varying—and sometimes negative—heat transfer coefficients (some of those results are surveyed in [37]). To the authors' knowledge, the role of the adiabatic wall temperature in microchannel heat transfer has not yet been systematically evaluated.

Most of the above-mentioned issues are commonly encountered in channels of conventional sizes, and it is recommended that single-phase heat transfer coefficients and pressure drops be calculated using conventional techniques, as found in [38] for example. Further review of the single-phase literature is given in [5].

Boiling Inception

In applications for which the coolant enters the channel in a subcooled state, the designer will want to consider the onset conditions for nucleate boiling, so that the cooling system will take advantage of the high heat transfer coefficients associated with subcooled boiling. The objective will be to reach subcooled boiling at the earliest point in the channel, without drying out the channel walls at the end of the channel; that is, without exceeding the critical heat flux for that flow. Stoddard et al. [39] reported conditions in which there is appreciable vapor quality at the end of a thin annulus, prior to CHF. In cases like that where there is an appreciable change in vapor quality over the length of the channel, the systems take advantage of even higher heat transfer coefficients in the convective boiling mode. However, the pressure drop is probably prohibitive.

Peng and colleagues reported numerous studies (e.g., [40, 41]) of small channels ($D_h = 0.15 - 0.64$ mm). The data are presented as semi-log plots of heat flux vs. wall temperature and heat transfer coefficient vs. wall temperature. Some rather interesting conclusions were drawn: laminar-turbulent transition occurs within the channel, with a consequent increase in the heat transfer coefficient; the coefficient was then approximately constant; at a relatively low wall superheat, the coefficient increased sharply, suggesting the inception of boiling; it was asserted that no partial nucleate boiling, or "knee" of the boiling curve, was encountered; and no evidence of boiling was observed in the channels, but vapor was observed in the exit headers. The last observation led to Peng's hypothesis of evaporating space and fictitious boiling. Regarding evaporating space, if the channel is too small, vapor formation is suppressed. The hypothesis of

---

[†]For example, for fully-developed laminar incompressible flow between two parallel adiabatic plates, $T_{\text{aw}} = T_b + (54/35)\Pr(u_b^2/2c_p)$.

fictitious boiling attempts to explain the heat flux that can be accommodated without apparent bubble formation. An additional incentive for this was the apparent lack of sufficient enthalpy rise of the liquid [41], although the earlier paper [40] reported an acceptable energy balance.

Some questions can be raised about these results. In the first place, multiple parallel channels (4 or 6) were used, and only the overall flow rate was measured; there is no way to deduce the flow rate in the individual channels. Secondly, the entire stainless steel test section was direct electrically heated, and the heat flux was stated as the heat generation (minus loss) divided by the surface area of the plate containing the machined channels. This apparently means that the reported heat flux is a factor of approximately 2 to 3 times less than the average heat flux at the channel walls. (Note that it is not clear what was actually done here, as earlier papers defined the heat flux in terms of the channel heated area.) Finally, the wall temperatures were recorded by thermocouples attached to the outside of the plate, which was then insulated, at the downstream end of the channels. These temperatures have only a casual relation to the temperatures of the channel walls, which vary circumferentially and axially. The net result is that it is very difficult to deduce boiling behavior from the data presented. Even with the simplified measurements, it was noted that there was "extreme difficulty in conducting the experiments" [41].

When plotted on a semi-log plot, the partial boiling regime is not very pronounced. This would show up better on a log-log plot. We suggest that partial boiling was likely present in the experiments reported in [40].

The lack of observed boiling in the channels warrants comment. The possibility of microscopic bubbles, undetected even with magnification, was mentioned by Peng et al. [40, 41]. Indeed, it is not unusual that the bubbles in forced subcooled boiling are very small and virtually undetectable [42]. This certainly could have been the case with the high subcoolings ($\approx 100°C$ for water) imposed in [40], even though the velocity was only about 1 m/s. Upon expanding into the exit plenum, where the velocity is greatly reduced, the very small bubbles could quickly agglomerate and become visible.

Recently, Peng et al. [43] argued that bubbles could be formed by density fluctuations (similar to homogeneous nucleation). They proposed that the density fluctuations (without phase change), or many growing and collapsing microscale bubbles, can absorb considerable energy, without change in enthalpy. This is the fictitious boiling hypothesis. Although it is difficult to see how this might happen without heat release during the collapse phase, these researchers have suggested that the process is like an endothermic chemical reaction.

Peng et al. [41] subsequently performed an analysis of bubble nucleation in microchannels. They derived bubble nucleation based on the stability of a vapor mass filling the small channel. Their criterion is

$$h_{lg}\alpha v_g/(c\pi v_{lg}qD_h) \leq 1 \qquad (34)$$

where c is an empirical constant relating to heat diffusion into the vapor mass.

The derived nucleation criterion is different from that developed for nucleation in conventional channels [44], but it does contain the channel hydraulic diameter: $q_{nucl} \sim 1/D_h$. Peng et al. [41] reported that initiation of boiling in microchannels requires extraordinarily high heat fluxes. The analytical results were taken as substantiation of the

concepts of evaporating space and fictitious boiling. If the microchannel size is smaller than the evaporating space, then fictitious boiling will be initiated before nucleation occurs.

For reference, let us examine the conventional model of flow-boiling nucleation from a spherical-sector cavity on the wall of the channel. According to [44], the radius of a cavity at incipient boiling is

$$r_c = (T_{\text{sat}} \, v_g \, 2\sigma \, k_l / h_{lg} q N)^{0.5} \tag{35}$$

assuming that cavities of all sizes are active (charged with a pre-existing gas phase and available for nucleation). The constant N refers to the distance from the wall at which the liquid temperature is equal to the required vapor temperature for stability of a spherical bubble in a superheated liquid. This is usually taken as $N = 1.0$; that is, the liquid everywhere below the bubble tip is able to transfer heat to the bubble, and cause it to go unstable.

A comparison of the two equations is given in Figure 6, for water at 1 atm — assuming $c = 1.0$ and $N = 1.0$. (A log-log plot is necessary, as the Cartesian plot of [41] does not capture the full range of heat flux.) At a heat flux of $q = 2.5 \times 10^5$ W/m^2, approximately the value at which nucleate-boiling behavior was observed in [40], the cavity diameter $(2r_c) \approx 0.014$ mm, which is well below the minimum wall dimension of 0.2 mm. It is concluded that bubble formation could have initiated from naturally occurring nucleation sites on the wall.

Rather than grow to fill the channel, the bubbles are torn from the wall before growing much larger, forming a bubble cloud, close to the wall where the liquid is superheated. With bubble diameters of the order of 10 micrometers, it is not surprising that they were not observed with a magnifying glass, especially since no bubbles were generated on the transparent cover plate. They would become visible, however, upon agglomeration in the exit header.

Regarding the lack of a concomitant enthalpy increase, as reported by Peng et al. [41], it is probable that the air exit in-fluid thermocouple encountered subcooled liquid rather than the true mixed-mean fluid.

The general conclusion is that nucleation from natural cavities should be possible for very small channels. This would be promoted by the roughness that is inherent in ver small channels, due to the manufacturing techniques utilized. (Note that in typical experiments with cover plates, the nucleation could occur due to small crevices between the cover and the test section, or at the gasket interfaces.) While channel size does not seem to be an issue for initiation of boiling in microchannels, the subsequent behavior of bubbles, at low or no subcooling, is expected to be strongly dependent on channel size.

Lopez and Ruggles [45] recently proposed and alternate criterion for nucleation, with fully developed laminar flow between parallel plates. They suggested that as the gap size decreases, nucleation is suppressed until very high heat fluxes are applied. This arises from considering the general interaction of the liquid and vapor temperature profiles and examining one of the resultant terms for saturated boiling. This term happens to contain channel size and wall heat flux, as shown below.

$$D_h = 32.94(T_{\text{sat}} \, v_g \, 2\sigma \, k_l / q \, h_{lg})^{0.5} \tag{36}$$

This equation, which is similar to Eq. (35) — except for the lead constant — is also plotted in Figure 6. This is to be interpreted as the heat flux required to initiate saturated boiling in a parallel-plate channel of given hydraulic diameter. It is evident, however, that there is a sharp disagreement between Eqs. (34) and (35), and even Eq. (36). We feel that Eq. (35) is the most accurate of the incipient boiling criteria, for both laminar and turbulent flow. Also, we feel that nucleation occurs at wall cavities, unless the channel size is really comparable to the cavity size, i.e., bubble growth in a cavity is restricted by the opposite channel wall.

The inception of boiling can be calculated from the intersection of the following expressions for forced convection and nucleation heat transfer, respectively:

$$q = h(T_w - T_b) = h\left[(T_w - T_{\text{sat}}) + (T_{\text{sat}} - T_b)\right] \tag{37}$$

$$q_{\text{nucl}} = \frac{(h_{lg})k_l(T_w - T_{\text{sat}})^2}{8T_{\text{sat}}v_g\sigma} \tag{38}$$

The onset of nucleate boiling is illustrated schematically in Figure 7, showing the intersection of Eqs. (37) and (38). The incipient boiling is followed by a transition to fully developed boiling, the so-called "knee" of the boiling curve. If it is advantageous to compute this region, the procedure is described in [44].

Flow Regimes

To date, there have been relatively few comprehensive studies of the effect of tube size on flow regimes in the size range of interest in this work. Coleman and Garimella [46] report observations of flow regimes in tubes of 1.3 to 5.5 mm diameter, but only for adiabatic air-water flows. They found distinct effects of diameter on flow regime transitions. This work is extended in a later paper, with a focus on intermittent flow [47]. A paper by Barnea et al. [48], which is cited in [19], looks at air-water flows in 2 to 6 mm tubes. A semi-empirical theory is developed. The effect of diameter is found to be small in this range. Tabatabai and Faghri [49] have proposed a new flow regime map for horizontal tubes, taking account of the influence of surface tension. A comparison to 1589 data points showed better performance than given by the well known Taitel-Dukler model within those regimes where surface tension affects the flow pattern. Extensive reviews of the existing literature are given by Kandlikar [3] and by Ghiaasiaan and Abdel-Khalik [4]. Until a need for full flow regimes maps surfaces, however, our knowledge in this area will probably remain incomplete.

Boiling Heat Transfer

Fully Developed Boiling

Fully Developed Subcooled Boiling. Since, as described above, we believe that nucleate boiling occurs at naturally occurring nucleation sites on the channel walls, it is reasonable to expect the fully developed boiling curves to be similar to those in regular channels. Few data are available, however. Peng and Wang [40] have some data for small

channels that suggest the q vs. $(T_w - T_{sat})$ relation is indeed similar to that for regular channels; but, they did not specify the pressure corresponding to their measurements.

Convective Boiling Heat Transfer.   Air-conditioning evaporators require the heat transfer coefficient for boiling with net vapor generation. Few data for small channels have been published in this regime. Zhao et al. [50] compared data for CO_2 in 0.86 mm triangular channels to five existing flow boiling correlations. The Kandlikar equation worked well for qualities below 40%, but the authors found that they could get within $\pm 20\%$ using a modified form of the Liu and Winterton equation. Kasza and Wambsganss [51] analyzed data for 2.26-mm circular channels, and concluded that nucleate-boiling bubbles were present at lower heat fluxes, where convective boiling is expected to dominate. They speculated that at higher heat fluxes, the bubbles agglomerate and slide along the surface — with the result that the q vs. $(T_w - T_{sat})$ relation is steeper than in the first region. In any case, only the first region would be of interest in air-conditioning. Visual studies (proposed) should be carried out, and comparisons need to be made with the predictions of conventional correlations.

Critical Heat Flux

The occurrence of CHF must be regarded as an undesirable condition, as it will cause overheating of an individual channel, or even the entire substrate containing the microchannels. There do not seem to be any data available for CHF in microchannels, so the best that can be done is look for CHF data in small-diameter tubes. Extensive experiments were conducted with tubes down to 0.3-mm diameter [52]. It was ascertained that CHF increased continuously as diameter was reduced to this value, other conditions remaining the same (see Figure 8).

The recent statistical correlation of Hall and Mudawar [53], using a very large subcooled boiling database, appears to account for the strong effect of tube diameter as the size is reduced below about 2 mm.

The critical heat flux (CHF) cannot increase indefinitely as the diameter is decreased from meso- to micro-scale, Figure 8. This diameter effect is speculated as being due to the greater influence of the bubble boundary layer for smaller diameters, [54]. As the diameter is reduced, the bubble boundary layer occupies a larger proportion of the cross-section, with a resulting increase in the velocity. For smaller diameters, the bubbles agglomerate and fill the channel, with the result that the CHF is caused by rupture of the liquid film between the bubble and the wall. The CHF in this case is expected to be lower than that for breakdown of the bubble boundary layer, and more random, due to the variation in the nucleation and agglomeration [55].

Consider data for saturated boiling on horizontal cylinders. The experiments of Sun and Lienhard [56] show that critical heat flux increases as diameter is decreased, according to the hydrodynamic stability theory. For very small cylinders, however, the theory breaks down. The resulting random behavior is associated with the way in which large bubbles behave after nucleation. In other words, a single bubble could trigger nucleation in pool boiling. An analogous erratic behavior could occur in channel flow; that is, a breakdown in the increasing CHF in Figure 8 would be expected at some very

small diameter. Given the small bubbles in subcooled boiling, however, this diameter is likely to be very small indeed.

Enhancement

There are several objectives that may be under consideration when heat transfer enhancement is applied to a thermal system. One of these objectives is to make a system smaller. Another is to achieve a larger heat duty for a given size. Consider the usual heat transfer rate equation:

$$Q = UA\Delta T \tag{39}$$

At fixed Q and ΔT, if the overall coefficient U is increased by enhancement, the heat exchange area, A, and overall size, can be reduced. Alternatively, for a fixed A and ΔT, an increased U will result in a larger Q.

We are concerned primarily with the latter situation. The heat exchangers will be made small through the application of microscale fabrication techniques. The objective is then to apply enhancement techniques to make them perform even better. An examination of the extensive literature in this field indicates, however, that virtually all enhancement techniques have been applied to compact and larger heat exchangers [57]. In other words, the enhancement (surface modification, inserts, externally powered devices) is rather large.

Of the many available techniques, fins would appear to be the most promising surface modification. However, the fin effectiveness may not be very high in view of the high heat transfer coefficients found in small channels. In addition, if the fins are small enough ("nanofins" perhaps), it is necessary to take into account the reduction of thermal conductivity that results from the scattering of the primary carriers of energy by the fin boundaries [10].

Surface-roughness effects are also a possibility. Most manufacturing processes introduce naturally surface roughness that may improve boiling heat transfer. This is expected to be mainly due to an increase in the active nucleation sites for flow nucleate boiling.

Kandlikar et al. [32] studied the effect of artificial roughness (acid etching) on heat transfer and flow friction. A roughness that had no effect on a 1.0-mm-diameter tube increased both the heat transfer coefficient and the friction factor for a 0.6-mm-diameter tube, due to the larger relative roughness in the smaller tube. A review of the literature indicated that the laminar-turbulent transition occurs at a lower Reynolds number as channel size is reduced. This could give an apparent enhancement in the transition region, as the heat transfer coefficient could be higher (i.e., turbulent) than expected on the basis of the transition Reynolds number for a larger channel.

There may be some fluid additives that prove beneficial, although they must not significantly affect the properties for which the working fluid was chosen in the first place. Heat transfer enhancement by outgassing of dissolved noncondensables, to create a boiling-like behavior in a single-phase fluid, is a possibility, e.g., water containing dissolved air [58]. (See note on flashing, in the introduction.) This effect dies out when boiling is established.

The tendency to use many parallel microchannels in order to manage pressure drop suggests a limiting condition of many very short channels oriented perpendicular to, rather than parallel to, the heated surface. This may take the form of circular or slot jets, with or without channel walls that function as fins between the jets. Such configurations can be made through a stacking of plates, with one or more plates representing the jet openings and other plates representing the fins (channel walls). This configuration simplifies the distribution of flow to headers on the order of the heated surface area. However, it tends to limit the microchannels to a single bank next to the heated surface. This configuration is best suited to cooling (for example of electronics), in which the coolant enters as single-phase liquid.

Flow Instability

The cooling systems used in a variety of electronic devices often consist of an array of parallel channels conveying the coolant through the heat sink. In order to design such a system using existing procedures, it is necessary to consider both the source of the data and its limitations. The most common experiment involves collecting heat transfer, and sometimes pressure drop, data on a flow-forced system using a single electrically heated round tube.

This procedure is flawed in that it fails to capture the Lednigg, or pressure-drop versus flow-rate instability, which can occur with subcooled boiling in channels [59, 64]. The manifestations of this instability consist of a deterioration that can lead to degraded heat transfer, or even a physical burnout. Usually, the deterioration is a result of one or more channels being starved for flow when a minimum in the pressure-drop-versus-flow-rate curve is reached. An oscillating solution is also possible if the flow delivery system is soft (compressible) enough (as shown for water in Figure 9 [60]). Similar flow instabilities have recently been reported for microchannel arrays [61, 62]. (The single tube experiment normally does not allow flow excursion because the system is flow forced, rather than fed from a constant pressure source.)

Some recent work [63] takes a closer look at this instability for heated test sections of various orientations and identifies the conditions which lead to it. It tends to appear at the point of significant vapor generation [64]. This is due to enhanced wall friction when subcooled boiling is present and an additional pressure drop due to the acceleration of the flow by the increasing void.

The key to predicting the onset of this flow instability is predicting the pressure drop versus flow rate curve. All terms have to be considered in the prediction: the orifice and entrance losses, the heated tube single-phase pressure losses, and the two-phase friction and momentum losses occurring near the end.

To summarize then, with many small boiling channels in parallel, the channels could be subject to an excursive instability, leading to critical heat flux (CHF). Alternatively, when there is a large compressible volume upstream there may be an oscillating flow leading to CHF [65]. More likely is an excursive instability where the overall system, having an essentially constant pressure drop from inlet to outlet header, interacts with the channel head-flow characteristic. In either case, the unstable condition is defined by the minimum in the channel head-flow curve [66]. This condition is illustrated for water in Figure 10.

The minimum is a result of the increased pressure drop due to subcooled boiling. Although it is not clear what the characteristics of subcooled boiling in microchannels are, there is a good possibility that a well-defined minimum in the head-flow curve will be observed. A procedure for correlating subcooled boiling pressure drop has been developed based on data for small channels [67]. This correlation, compared with water data in Figure 11, is:

$$\Delta p = (\Delta p_{\text{lo}}^n + \Delta p_{\text{sb}}^n)^{1/n} \tag{40}$$

where any gravitational component has been subtracted from the measured pressure drop. The procedure for correlating the single-phase and subcooled-boiling contributions is outlined in [67]. It is noted that the correlation can also be plotted as pressure drop vs. flow rate, so that a minimum can be easily spotted for a given Δp. The heat flux corresponding to this minimum is the expected CHF.

It is recommended that such correlations be obtained for microchannels. The hydro-dynamically defined CHF is quite a bit lower than the stable CHF that would be obtained in a single channel having a constant flow rate.

A stable solution can be assured with a sufficiently large inlet orifice pressure drop in each tube, even for an array of parallel channels. Fabrication and evaluation techniques for these orifices need to be developed for very small channels. Another possibility that should be investigated is pressure-drop oscillation caused by the internal compressibility of very long channels ($L/D > 150$). Microchannels may well exceed this length; however, the effect has only been demonstrated in conventional channels.

Manufacturing Challenges

Finally we comment on the manufacturability of systems like we described here. Manufacturing a large number of tiny parallel channels of specified length is achievable through semiconductor manufacturing techniques. Of perhaps greater concern is the need to split the flow uniformly among the parallel channels, and to assure stability of this distribution (which was discussed earlier in this paper). If we envision the traditional method of putting an orifice at the entrance of each channel, this could pose a manufacturing challenge.

In order to maintain flow stability, it would be important for each orifice to be the same as all the others, both in geometry and placement. The orifice will necessarily be smaller than the channels, and therefore require a tighter manufacturing tolerance than the channels themselves. The orifice is etched into one layer of the stack or into a separate layer joined at 90 degrees to the stack.

Another challenge is the actual layout of the many parallel channels, with the necessity to bring fluid into channel entrances that may necessarily be distributed over the heating surface area, rather than at one end. While there has been impressive progress in precision flow splitting into many microchannels, this was done in polymers rather than in silicon. Bowman and Maynes [68] review fabrication methods for microchannel heat exchangers.

Conclusions and Recommendations

Conclusions

1. As with single-phase cooling systems, the use of smaller channel diameters for phase-change-dominated cooling systems generally results in a smaller system size, without necessarily imposing a larger pumping power requirement, as compared to a system with larger channel diameters, with the same total mass flow rate and heat removal rate. The smaller systems will have many parallel channels of relatively short length, as compared with the larger system.

2. Conduction resistance in the channel walls can, in principle, be a smaller contributor to the total thermal resistance than the convective thermal resistance; however, in designs that involve thin solid sections (such as rows of rectangular channels), significant fin effects are to be expected. Since manufacturing processes tend to favor such layouts, optimization of the channel depth and width relative to the solid thickness will be desirable in order to limit such fin resistance.

3. Fin effects in straight sections of rectangular channel walls can reasonably be modeled using one-dimensional fin analyses in cases where the fin efficiency is above 80%.

4. Heat conduction effects around channel walls may tend to inhibit the occurrence of burnout during CHF in small channels. This possibility must be evaluated in the context of specific heat loads and flow conditions.

5. Flow distribution for single-phase flows and subcooled boiling can be handled using existing methods, with the caution that tight control on the dimensions and workmanship are essential if the distribution system is to work as designed.

6. Single-phase heat transfer coefficients in small channel arrangements should be computed using the same results as for conventional systems. Particular care must be exercised in accounting for entry-length effects, surface roughness, nonuniformities in the thermal conditions at the channel wall. When viscous dissipation is significant, the adiabatic wall temperature should be used in calculating wall heat flux; and for liquids (but not gases) the bulk temperature variation must be corrected for dissipation.

7. An analysis was performed to show that incipient boiling in a subcooled, forced-convection flow most likely is governed by nucleation sites on the channel walls, and is not tied-in with the channel dimensions. The bubbles in water are only of the order of 10 micrometers in diameter; hence, they are not visible in the channel. However, on leaving the channel, they would be expected to agglomerate and become visible to the naked eye.

8. Comprehensive understanding of flow regimes in small diameter heated tubes has not yet been realized. No compelling need for this knowledge has appeared yet either.

9. The data for subcooled boiling and convective boiling in very small channels are very limited.

10. It is expected that fully developed subcooled boiling in microchannels is the same as in regular channels.

11. In the absence of critical heat flux (CHF) data for microchannels, small-tube data must be relied upon. The subcooled CHF increases as diameter is reduced. A speculation is advanced that this will not continue indefinitely; at some very small diameter, the CHF will decrease and be quite random.

12. Aside from surface roughness, which is usually a natural result of the fabrication technique, and fins, enhancement technology has been limited to relatively large, conventional heat exchangers. There would, however, be benefits to improving heat transfer in all modes encountered in microchannels. In particular, the necessity of large numbers of small parallel channels suggests that designers consider circular or slot jet arrangements as an alternate to the challenge of accurate flow splitting into multiple parallel channels.

13. Excursive instability will be encountered in parallel-channel micro heat exchangers with subcooled boiling. Inlet orificing will be required to raise the critical heat flux above that corresponding to the minimum in the channel pressure drop/flow rate curve at the supply pressure drop.

Recommendations

1. Data are needed for subcooled boiling and convective boiling heat transfer and pressure drop, and for critical heat flux, in channels with hydraulic diameters smaller than 0.3 mm. Comparisons with this data and conventional correlations are also needed. Correlations should be developed for subcooled boiling pressure drop that allow determination of the hydrodynamic critical heat flux.

2. Visualization of flow boiling in channels with transparent cover plates should be made with a microscope in order to detect very small bubbles.

3. Enhancement methods should be developed for flow boiling in very small heat exchangers.

Acknowledgment

Nomenclature

A	heat exchange area (m^2)
Bi	Biot number, hD_h/k_{solid}
C	ratio of orifice pressure drop to channel pressure drop
c_{p_l}	specific heat of liquid coolant (J/kg·K)
D	channel diameter or width (m)
D_h	hydraulic diameter (m)
f	Darcy friction factor
H	length = width of heater (m)
h	heat transfer coefficient (W/m^{2}K)
h_b	bulk enthalpy of fluid (J/kg)
h_{lg}	latent heat of vaporization of fluid (J/kg)
k_{fluid}	thermal conductivity of coolant (W/m·K)
k_l	thermal conductivity of liquid (W/m·K)
k_{solid}	thermal conductivity of solid (W/m·K)
L	length of flow channel (m)
M	mass flow rate of coolant (kg/s)
m	fin parameter (m^{-1})
N	constant for bubble stability condition
n	number of channels
n_c	number of channels in a row
n_h	number of holes in a cross section
Nu$_D$	Nusselt number, hD_h/k_{fluid}
P	pumping power (W)
Pr	Prandtl number
Q	heat rate (W)
q	average channel wall heat flux (W/m^2)
q_0	fixed upper surface heat flux (W/m^2)

q_{CHF}	critical heat flux (W/m^2)
q_{nucl}	nucleate boiling heat flux(W/m^2)
r	ratio of channel length to block length, $r = L/H$
r_c	cavity radius (m)
S	ratio of channel spacing to channel width
T	temperature (K)
T_0	fixed upper surface temperature (K)
T_{aw}	adiabatic wall temperature (K)
T_b	local bulk temperature (K)
T_{CHF}	temperature of surface at CHF (K)
T_{max}	maximum tube wall temperature (K)
T_{sat}	saturation temperature of fluid (K)
T_{sub}	inlet temperature of subcooled coolant (K)
t_c	thickness of rectangular channel (m)
t_s	thickness of fin (m)
u_b	bulk velocity (m/s)
U	overall heat transfer coefficient (W/m^{2}K)
v_g	specific volume of vapor (m^3/kg)
v_{lg}	specific volume of vapor minus specific volume of liquid (m^3/kg)
W	thickness of heating block (m)
W_b	distance from heated surface to channel center (m)
W_c	length of long side of rectangular channel (m)
x	exit quality of coolant
z	axial dimension of the channel (m)
α	thermal diffusivity (m^2/s)
β	value of laminar Nusselt number
Δp	pressure drop through channels (Pa)
Δp	total pressure drop (Pa)

Δp_{ent}	pressure drop at the entrance of the channel (Pa)
Δp_{lo}	frictional pressure drop of equivalent single-phase liquid flow along the channel (Pa)
Δp_{fr}	frictional pressure drop of two-phase flow along the channel (Pa)
Δp_{sb}	pressure drop attributed to subcooled boiling (Pa)
Δx	change in vapor quality of coolant over the length of the channel
ρ_l	liquid density (kg/m^3)
ρ_g	vapor density (kg/m^3)
σ	surface tension (N/m)
Φ_l	ratio of two-phase pressure drop to single-phase liquid pressure drop

References

[1] McDonald, C.F., Low Cost Compact Primary Surface Recuperator Concept for Microturbines, *Applied Thermal Engineering*, vol. 20, pp. 471–497, 2000.

[2] Mehendale, S.S., Jacobi, A.M., and Shah, R.K., Fluid Flow and Heat Transfer at Micro- and Meso-Scales with Application to Heat Exchanger Design, *Applied Mechanics Reviews*, vol. 53, no. 7, pp. 175–193, 2000.

[3] Kandlikar, S.G., Two-phase Flow Patterns, Pressure Drop, and Heat Transfer during Boiling in Minichannel Flow Passages of Compact Evaporators, *Heat Transfer Engineering*, vol. 23, pp. 5–23, 2002.

[4] Ghiaasiaan, S.M., and Abdel-Khalik, S.I., Two-phase Flow in Microchannels, *Advances in Heat Transfer*, vol. 34, pp. 145–254, 2001.

[5] Garimella, S. V., and Sobhan, C. B., Transport in Microchannels — A Critical Review, *Ann. Rev. Heat Transfer* (to appear), 2002.

[6] Majumdar, A., Peterson, G.P., and Poulikakos, D., Micro/Nanoscale Heat Transfer, special issue of *J. Heat Transfer*, vol. 124, pp. 221–401, 2002.

[7] Whalley, P.B., *Boiling, Condensation, and Gas-Liquid Flow*, Oxford University Press, Oxford, 1987.

[8] Bowers, M.B., and Mudawar, I., High Flux Boiling in Low Flow Rate, Low Pressure Drop Mini-channel and Micro-channel Heat Sinks, *Intl. J. Heat Mass Transfer*, vol. 37, pp. 321–332, 1994.

[9] Palm, B., Heat Transfer in Microchannels, *Heat Transfer and Transport Phenomema in Microscale*, G.P. Celata (ed.), Begell House, New York, pp. 54–64, 2000.

[10] Chou, F.C., Lukes, J.R., and Tien, C.-L., Heat Transfer Enhancement by Fins in the Microscale Regime, *J. Heat Transfer*, vol. 121, pp. 972–977, 1999.

[11] Bowers, M.B., and Mudawar, I., Two-phase electronic cooling using mini-channel and micro-channel heat sinks - Part 1. Design criteria and heat diffusion constraints, *Advances in Electronic Packaging*, *J. Electronic Packaging*, vol. 116, pg. 290–297, 1994.

[12] Phillips, R.J., Forced-convection liquid-cooled microchannel heat sinks, Technical Report 787, MIT Lincoln Laboratory, Lexington MA, 7 January 1988.

[13] Kadle, D.S., and Sparrow, E.M., Numerical and experimental study of turbulent heat transfer and fluid flow in longitudinal fin arrays, *J. Heat Transfer*, vol. 108, no. 1, pp. 16–23, 1986.

[14] Lienhard V, J.H., and Lienhard IV, J.H., *A Heat Transfer Textbook*, 3rd ed., Phlogiston Press, Cambridge MA, http://web.mit.edu/lienhard/www/ahtt.html, 2002.

[15] Phillips, R.J., Glicksman, L., and Larson, R., Forced Convection, Liquid-cooled Microchannel Heat Sinks for High-power Density Microelectronics, *Cooling Technology for Electronic Equipment*, W.Aung (editor), Hemisphere Publishing Corp., New York, pp. 295–316, 1988.

[16] Tuckerman D.B., and Pease, R.F.W., High performance heat sinking for VLSI, *IEEE Electron Device Letters*, vol. EDL-2, pp.126–129, 1981.

[17] Rostami, A.A., Hasan, A.Y., and Chia, S.L., 2000, "Conjugate heat transfer in microchannels," , *Heat Transfer and Transport Phenomema in Microscale*, G.P. Celata (ed.), Begell House, New York, pp. 121–128, 2000.

[18] Fedorov, A.G., and Viskanta, R., Three-dimensional conjugate heat transfer in the microchannel heat sink for electronic packaging, *Intl. J. Heat Mass Transfer*, vol. 43, pp. 399–415, 2000.

[19] Idelchik, I.E., *Handbook of Hydraulic Resistance*, 2nd ed., Chpt. 7, Hemisphere Publishing Corp., New York, 1986.

[20] Smith, H.G., Design of a test apparatus to analyze two-phase refrigerant flow in furnace coil applications, S.M. Thesis in Mechanical Engineering, Massachusetts Institute of Technology, Cambridge MA, June 1995.

[21] Chen, S.S., Refrigerant distribution model development, S.M. Thesis in Mechanical Engineering, Massachusetts Institute of Technology, Cambridge MA, June 1995.

[22] Perkins, R., Air-water modeling of refrigerant distribution tripods, S.B. Thesis in Mechanical Engineering, Massachusetts Institute of Technology, Cambridge MA, March 1997.

[23] Quintanta, M.S., Two-phase flow splitting in piping branches, S.M. Thesis in Nuclear Engineering, Massachusetts Institute of Technology, Cambridge MA, June 1998.

[24] Hrnjak, P., Refrigerant distribution and charge reduction in micro channel evaporators and condensers, presentation at ASHRAE Annual Meeting, Honolulu, 24 June 2002.

[25] Zietlow, D., Compagna, M., and Dias, M., Innovative experimental apparatus to measure liquid flow distribution in two-phase flow occurring in manifolds of compact heat exchangers, presentation at ASHRAE Annual Meeting, Honolulu, 23 June 2002.

[26] Hadjiconstantinou, N.G., Convective heat transfer in micro and nano channels: Nusselt number beyond slip flow, *Proc. ASME Heat Transfer Division*, vol. 366-2, pp. 13–22, 2000.

[27] Obot, N.T., Toward a better understanding of friction and heat/mass transfer in microchannels - A literature review, *Microscale Thermophysical Engineering*, vol. 6, pp. 155–173, 2002.

[28] Sobhan, C.B., and Garimella, S.V., A comparative analysis of studies on heat transfer and fluid flow in microchannels, *Microscale Thermophysical Engineering*, vol. 5, pp. 293–311, 2001.

[29] Kawaji, M., Chung, P.M.-Y., and Kawahara, A., Instantaneous Velocity Profiles and Characteristics of Pressure-Driven Flow in Microchannels, *Proc. 2001 ASME IMECE*, Paper No. HTD-24209, New York, 11-16 November 2001.

[30] Judy, J., Maynes, D., and Webb, B.W., Liquid Flow Pressure Drop in Microtubes, , *Heat Transfer and Transport Phenomema in Microscale*, G.P. Celata (ed.), Begell House, New York, pp.149–154, 2000.

[31] Liu, D., and Garimella, S.V., Investigation of Liquid Flow in Microchannels, *8th AIAA/ASME Joint Thermophysics Heat Transfer Conf.*, St. Louis, 24–26 June 2002.

[32] Kandlikar, S.G., Joshi, S., and Tiau, S., Effect of Channel Roughness on Heat Transfer and Fluid Flow Characteristics at Low Reynolds Numbers in Small Diameter Tubes, *Proc. 2001 National Heat Transfer Conf.*, Anaheim, CA, 10–12 June 2001.

[33] Turner, S.E., Sun, H., Faghri, M., and Gregory, O.J., Effect of surface roughness on gaseous flow through microchannels, *Proc. ASME Heat Transfer Division - 2000*, HTD-Vol. 366-2, pp.291–298, 2000.

[34] Shapiro, A.H., *The Dynamics and Thermodynamics of Compressible Fluid Flow*, Ronald Press, New York, 1953.

[35] Kedzierski, M.A., Micro channel heat transfer and macro channel prediction methods, presentation at ASHRAE Annual Meeting, Honolulu, 24 June 2002.

[36] McAdams, W.H., Nicolai, L.A., Keenan, J.H., Measurements of recovery factors and coefficients of heat transfer in a tube for subsonic flow of air, *Trans. AIChE*, vol. 42, pp. 907–925, 1946.

[37] Shah, R.K., and London, A.L., Laminar flow forced convection in ducts, *Advances in Heat Transfer*, Suppl. 1, Academic Press, New York, 1978.

[38] Kakac, S., Shah, R.K., and Aung, W., (editors), *The Handbook of Single-Phase Convective Heat Transfer*, John Wiley & Sons, New York, 1987.

[39] Stoddard, R.M., Dowling, M.F., Abdel-Khalik, S.I., Ghiaasiaan, S.M., and Jeter, S.M., Critical heat flux in heated horizontal thin annuli, *Proc. ASME Intl. Mech. Engr. Congress and Exposition*, ASME, New York, 2000.

[40] Peng, X.F. and Wang, B.X., Cooling Characteristics with Microchanneled Structures, *Enhanced Heat Transfer*, vol. 1, pp. 315–326, 1994.

[41] Peng, X.F., Hu, H.Y., and Wang, B.X., Boiling Nucleation During Liquid Flow in Microchannels, *Intl. J. Heat Mass Transfer*, vol. 41, pp. 101–106, 1998.

[42] Vandervort, C.L., Bergles, A.E., and Jensen, M.K., Heat Transfer Mechanisms in Very High Heat Flux Subcooled Boiling, *Fundamentals of Subcooled Boiling*, vol. 217, ASME, New York, pp. 11–17, 1992.

[43] Peng, X.F., Tien, Y., and Lee, D.J., Arguments on Microscale Boiling Dynamics, , *Heat Transfer and Transport Phenomema in Microscale*, G.P. Celata (ed.), Begell House, New York, pp.186–190, 2000.

[44] Bergles, A.E. and Rohsenow, W.M., The Determination of Forced-Convection Surface-Boiling Heat Transfer, *J. Heat Transfer*, vol. 86, pp. 365–372, 1964.

[45] Lopez, M., and Ruggles, A.E., Onset of Vapor Generation in Small Channels at Low Reynolds, , *Heat Transfer and Transport Phenomema in Microscale*, G.P. Celata (ed.), Begell House, New York, pp. 179–185, 2000.

[46] Coleman, J.W., and Garimella, S., Characterization of two-phase flow patterns in small diameter round and rectangular tubes, *Intl. J. Heat Mass Transfer*, vol. 42, pp. 2869–2881, 1999.

[47] Garimella, S., Killion, J.D., and Coleman, J.W., An Experimentally Validated Model for Two-phase Pressure Drop in the Intermittent Flow Regime for Circular Microchannels, *Proc. ASME NHTC 2001*, Anaheim, 10–12 June 2001.

[48] Barnea, D., Luninsky, Y., and Taitel, Y., Flow Patterns in Horizontal and Vertical Two-Phase Flow in Small Diameter Pipes, *Canadian J. Chem. Engr.*, vol. 61, pp. 617–620, 1983.

[49] Tabatabai, A., and Faghri, A., A New Two-Phase Flow Map and Transition Boundary Accounting for Surface Tension Effects in Horizontal Miniature and Micro Tubes, *J. Heat Transfer*, vol. 123, pp. 958–968, 2001.

[50] Zhao, Y., Molki, M., and Ohadi, M.M., Predicting Flow Boiling Heat Transfer of CO_2 in Microchannels, *Proc. 2001 ASME IMECE*, Paper no. HTD-24216, New York, 11–16 November 2001.

[51] Kasza, K. E. and Wambsganss, M. W., Development of a Small-Channel Nucleate Boiling Heat Transfer Correlation, Argonne National Laboratory Report ANL-94/32, 1994.

[52] Vandervort, C.L., Bergles, A.E., and Jensen, M.K., An Experimental Study of Critical Heat Flux in Very High Heat Flux Subcooled Boiling, *Intl. J. Heat Mass Transfer*, vol. 37, Suppl. 1, 161–173, 1994.

[53] Hall, D.D. and Mudawar, I., Critical Heat Flux (CHF) for Water Flow in Tubes - II, Subcooled CHF Correlations, *Intl. J. Heat Mass Transfer*, vol. 43, pp. 2605–2640, 2000.

[54] Bergles, A.E., Subcooled Burnout in Tubes of Small Diameter, ASME Paper No. 63-WA-182, 1963.

[55] Fiori, M.P., and Bergles, A.E., Model of Critical Heat Flux in Subcooled Flow Boiling, *Heat Transfer 1970, Proc. 4th Intl. Heat Transfer Conf.*, Elsevier Publishing Co., Amsterdam, vol. 6, Paper B6.3, 1970.

[56] Sun, K.H., and Lienhard IV, J.H., The Peak Pool Boiling Heat Flux on Horizontal Cylinders, *Intl. J. Heat Mass Transfer*, vol. 13, p. 1425–1439, 1970.

[57] Bergles. A.E., New Frontiers in Enhanced Heat Transfer, *Advances in Enhanced Heat Transfer - 2000*, ASME, New York, NY, HTD-vol. 365, pp. 1–8, 2000.

[58] Adams, T.M., Ghiaasiaan, S.M., and Abdel-Khalik, S.I., Enhancement of Liquid Forced Convection Heat Transfer in Microchannels Due to the Release of Non-condensables, *Intl. J. Heat Mass Transfer*, vol. 42, pp. 3563–3573, 1999.

[59] Hetsroni, G., *Handbook of Multiphase Flow*, Hemisphere Publishing Corp., Washington DC, pp. 2-95 to 2-136, 1982.

[60] Maulbetsch, J.S. and Griffith, P., System-Induced Instabilities in Forced Convection Flows with Subcooled Boiling, *Proc. 3rd Intl. HT Conference*, Chicago, vol. 4, pp. 247–257, 1966.

[61] Hetsroni, G., Mosyak, A., Segal, Z., Two-phase Flow in Microchannels, *Proc. 2001 ASME IMECE*, Paper No. HTD-24216, New York, 11–16 November 2001.

[62] Kandlikar, S.G., Steinke, M.E., Tian, S., and Campbell, L.A., High-Speed Photographic Observation of Flow Boiling of Water in Parallel Mini-Channels, *Proc. 2001 National Heat Transfer Conf.*, Anaheim, CA, 10–12 June 2001.

[63] Babelli, I. and Ishii, M., Flow Excursion Instability in Downward Flow Systems: Part II Two-Phase Instability, *Nuclear Engr. Design*, vol. 206, pp. 97–104, 2001.

[64] Tong, L.S. and Tang, Y.S., *Boiling Heat Transfer and Two Phase Flow*, Taylor and Francis, Washington DC, pp. 457–480, 1997.

[65] Daleas, R.S. and Bergles, A.E., Effects of Upstream Compressibility on Subcooled Critical Heat Flux, ASME Paper No. 65-HT-67, ASME, New York, 1965.

[66] Boure, J.A., Bergles, A.E., and Tong, L.S., Review of Two-Phase Flow Instability, *Nuclear Engr. Design*, vol. 25, pp. 165–192, 1973.

[67] Pabisz, R.A., Jr. and Bergles, A.E., Using Pressure Drop to Predict the Critical Heat Flux in Multiple Tube, Subcooled Boiling Systems, *Experimental Heat Transfer, Fluid Mechanics and Thermodynamics*, vol. 2, Edizioni ETS, Pisa, Italy, 1997, pp. 851–858, 1997.

[68] Bowman, W.J. and Maynes, D., A Review of Micro Heat Exchanger Flow Physics, Fabrication, Methods, and Applications, *Proc. 2001 ASME IMECE*, Paper No. HTD-24216, New York, 11–16 November 2001.

List of Tables

Table 1: Dimensionless azimuthal temperature differences for $W = S \times D = 2W_b$

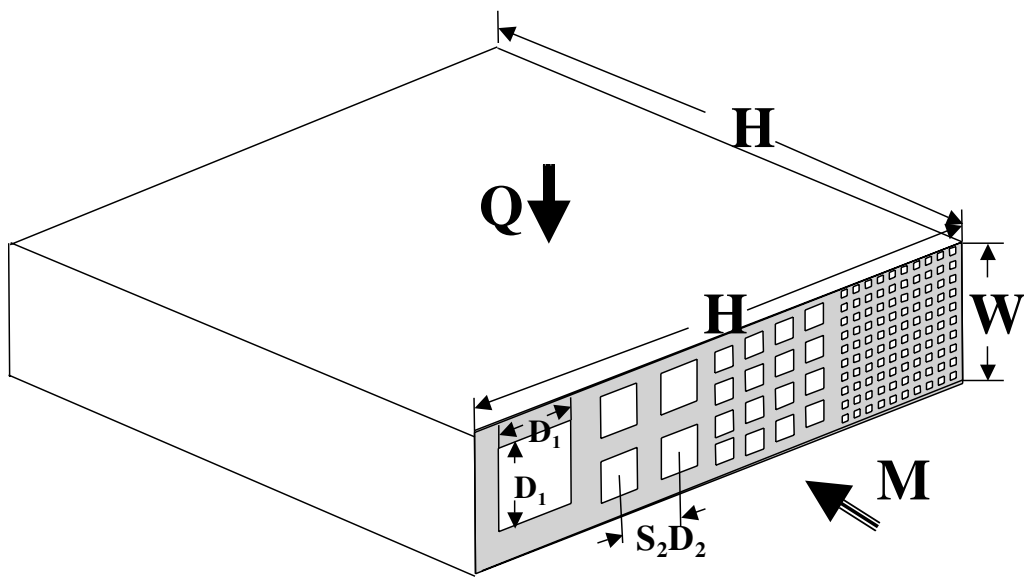|	D/W							
	0.1	0.2	0.3	0.4	0.5	0.6	0.7	0.8
q_0 *fixed*	0.64	0.79	1.0	1.3	1.62	2.1	2.7	3.8
T_0 *fixed*	0.39	0.52	0.66	0.77	0.86	0.93	0.97	0.99

List of Figures

Figure 1 Flow configurations.
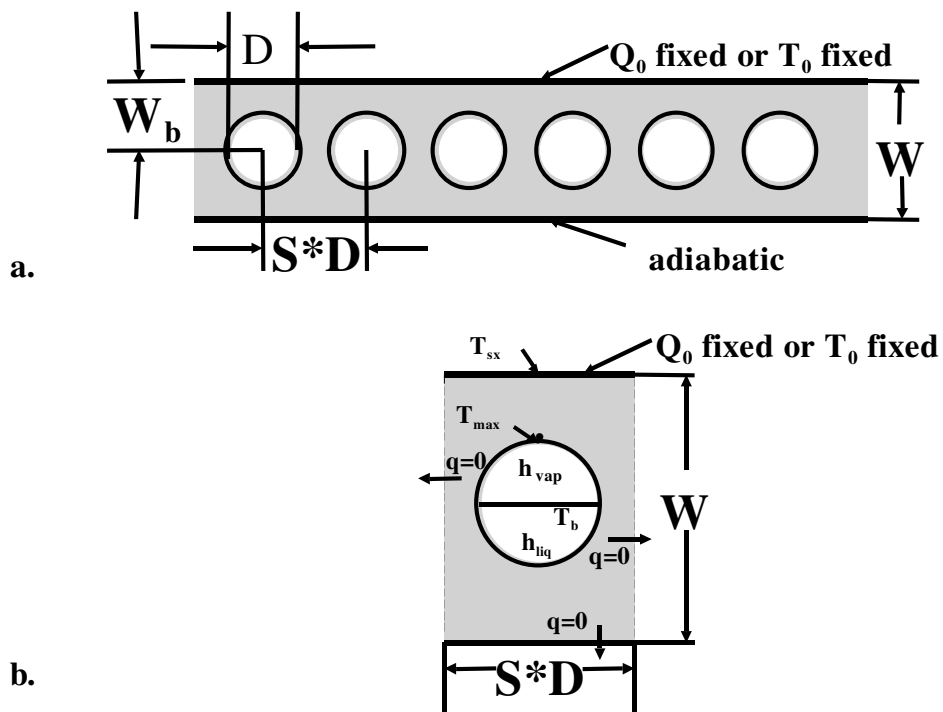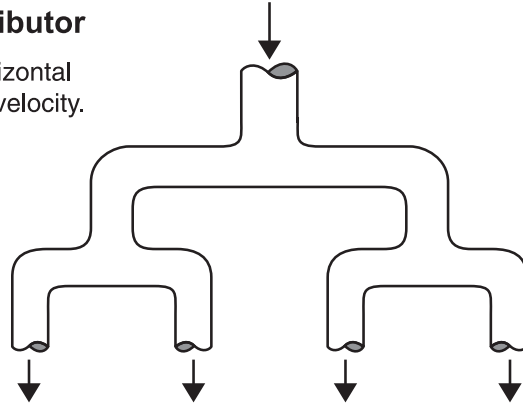
Figure 2   Geometry for conjugate effects.
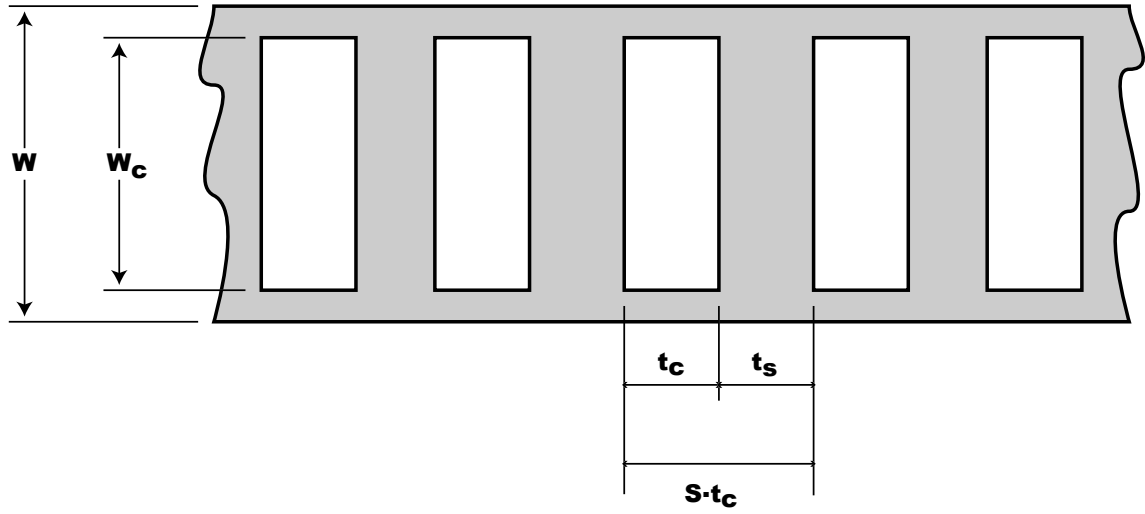
Figure 3 Rectangular channel geometry.

A. Branching distributor

Either place in a horizontal
plane or use a high velocity.

B. Circular distributor

Either put this in a vertical
plane or use a high velocity.

A

A

Section B-B

Section A-A

B

B
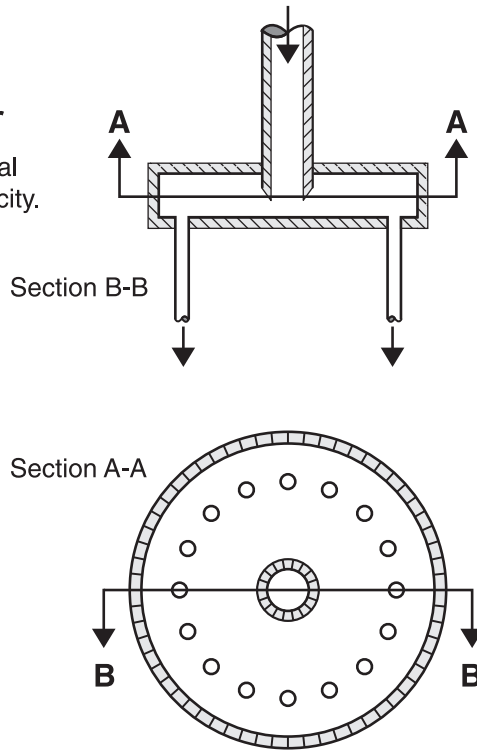
Figure 4   Two phase flow distributors.
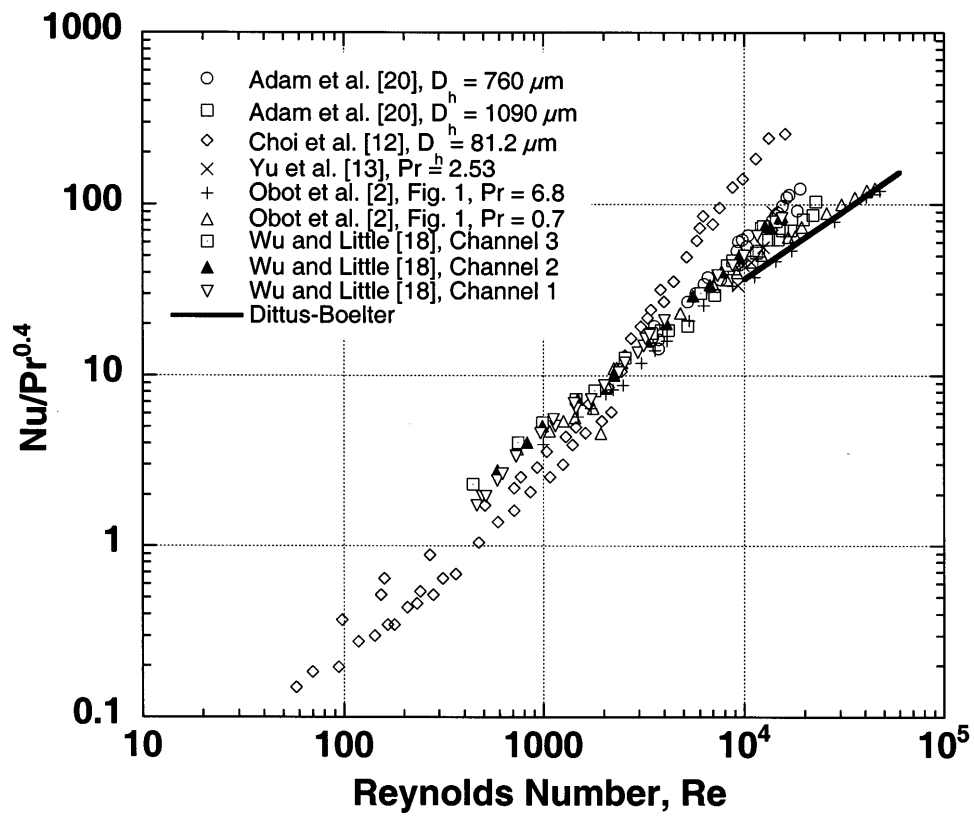
Figure 5 Nusselt numbers measured in microchannels scaled against Reynolds and Prandtl numbers (Courtesy of N. Obot: [27], revised).
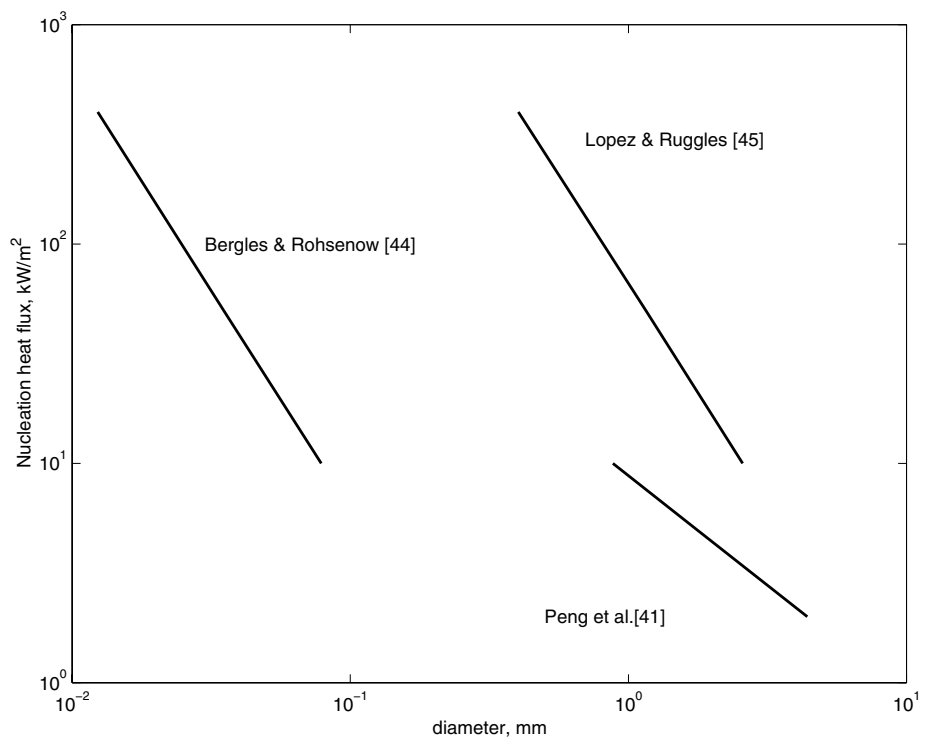
Figure 6 Nucleation heat flux for water (diameter: B& R, cavity diameter; P, L& R, channel diameter).
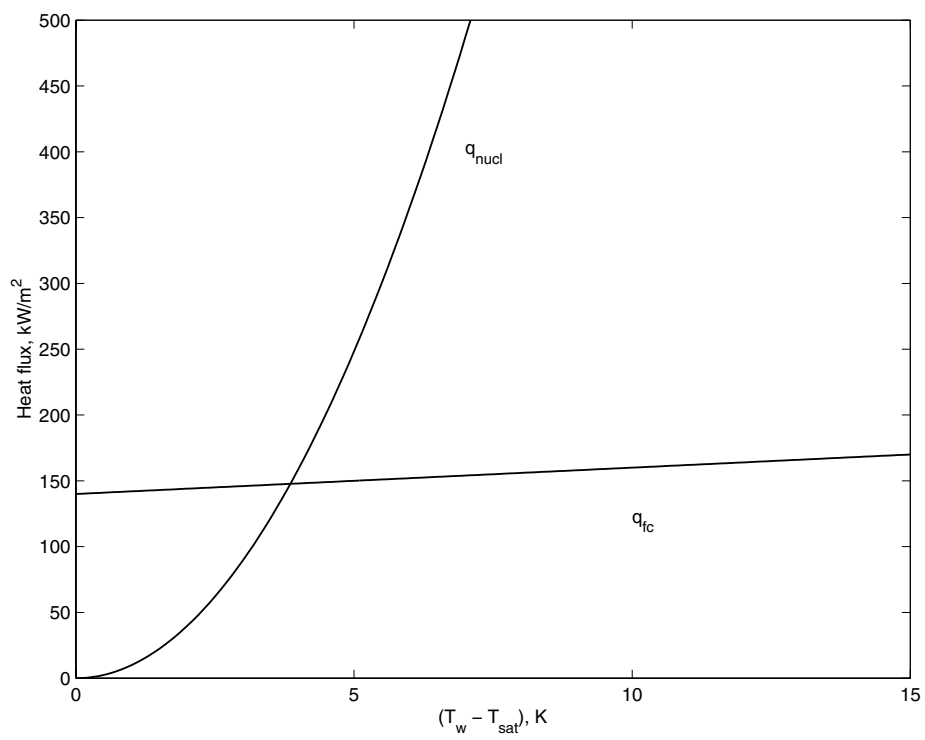
Figure 7 Onset of boiling for water at 2 MPa with 70 K subcooling ($h = 2000$ W/m^{2}K).
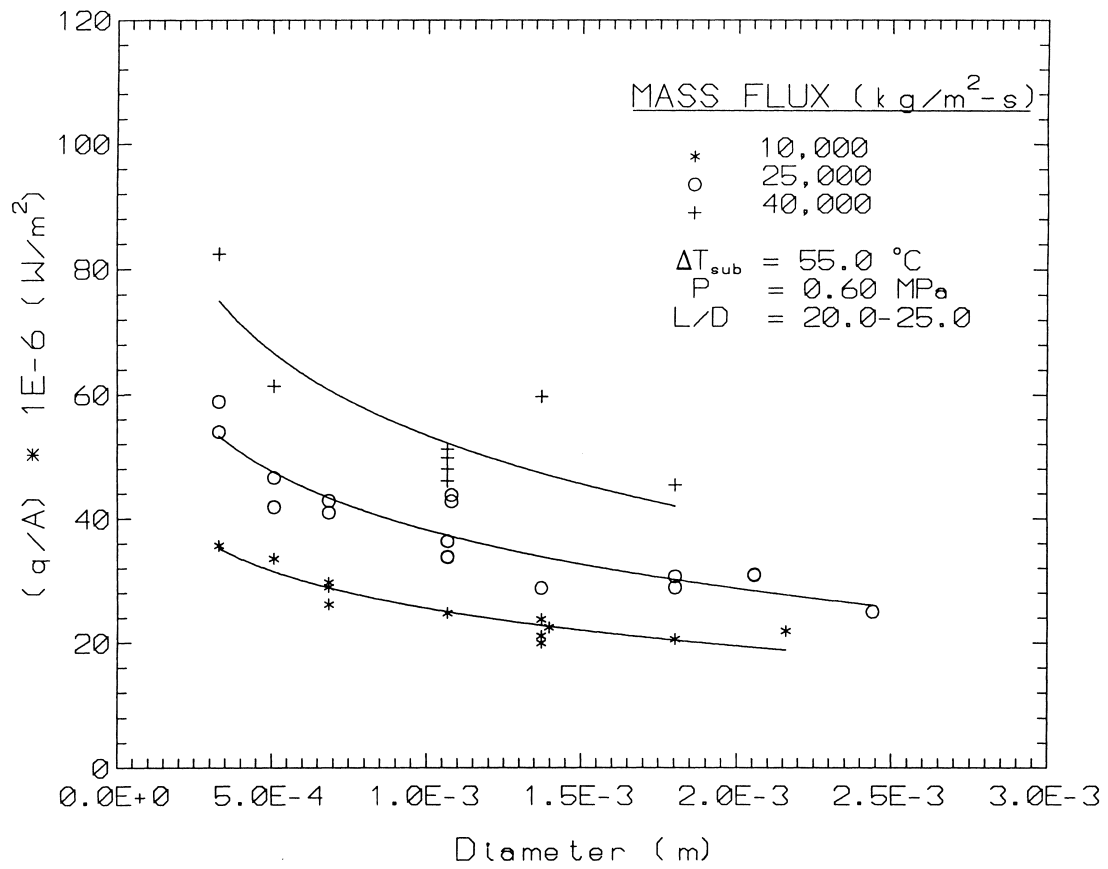
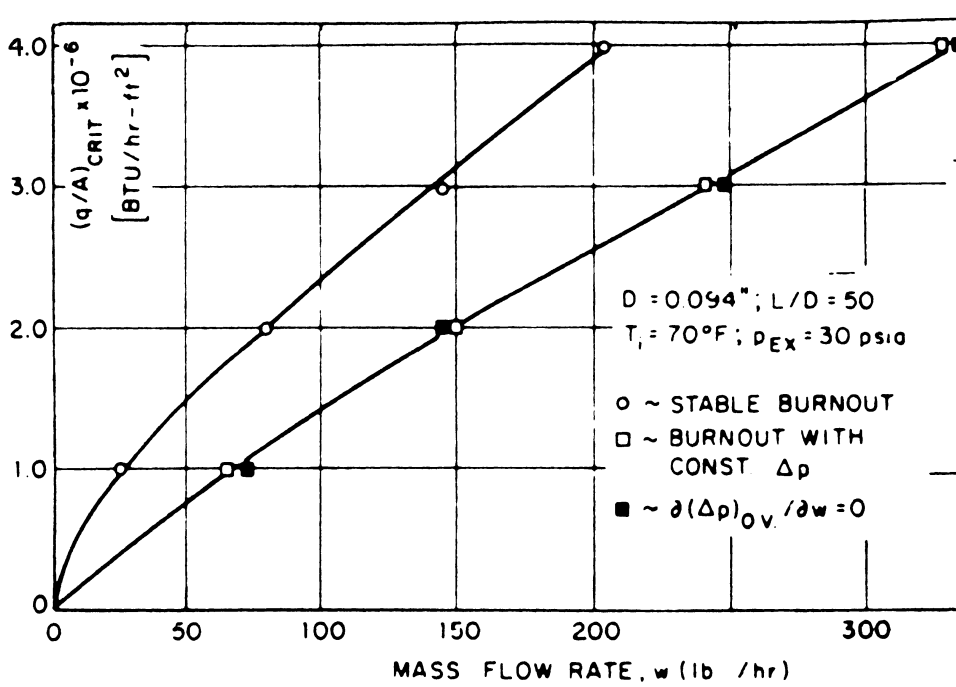**Figure 8** Dependence of critical heat flux on channel diameter for water.

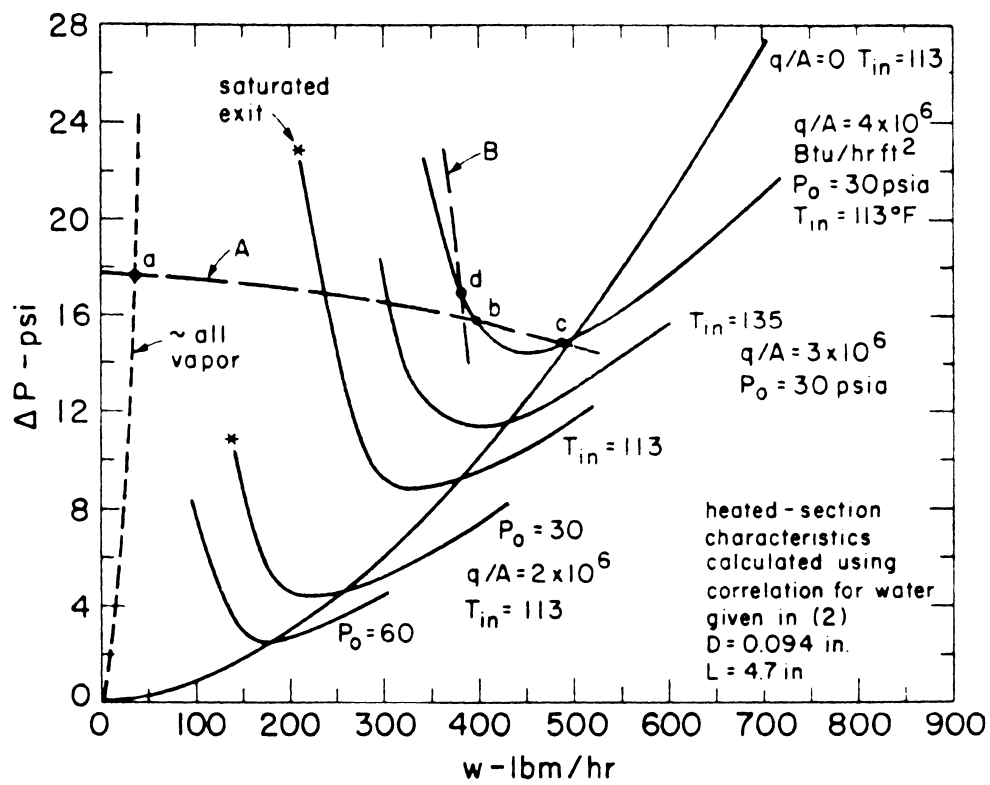**Figure 9** Stable and unstable critical heat flux for water.
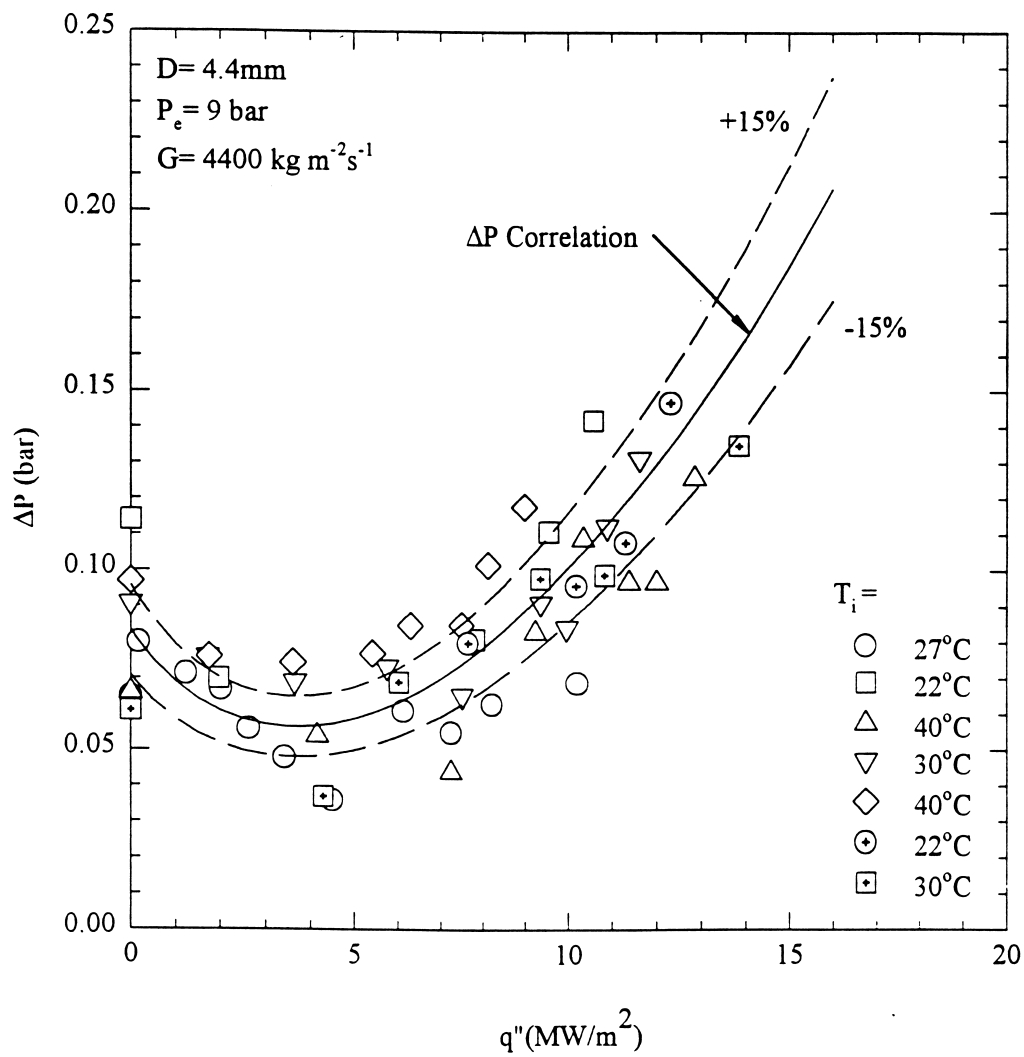
Figure 10 Flow rate dependence of subcooled boiling pressure drop.

Figure 11 Pressure drop for subcooled boiling of water.